Tellus (2007), 59B, 77–98

Blackwell Munksgaard, 2006

TELLUS

Interannual variation and trends in air pollution over Europe due to climate variability during 1958–2001 simulated with a regional CTM coupled to the ERA40 reanalysis

By CAMILLA ANDERSSON[1,2]*, JOAKIM LANGNER[2] and ROBERT BERGSTRÖM[2],
[1]*Department of Applied Environmental research, Stockholm University, SE-10691 Stockholm, Sweden;* [2]*Swedish Meteorological and Hydrological Institute, SE-60176 Norrköping, Sweden*

(Manuscript received 23 December 2005; in final form 13 June 2006)

ABSTRACT

A three-dimensional Chemistry Transport Model was used to study the meteorologically induced interannual variability and trends in deposition of sulphur and nitrogen as well as concentrations of surface ozone (O_3), nitrogen dioxide (NO_2) and particulate matter (PM) and its constituents over Europe during 1958–2001. The model was coupled to the meteorological reanalysis ERA40, produced at the European Centre for Medium-range Weather Forecasts. Emissions and boundary conditions of chemical compounds and PM were kept constant at present levels.

The average European interannual variation, due to meteorological variability, ranges from 3% for O_3, 5% for NO_2, 9% for PM, 6–9% for dry deposition, to about 20% for wet deposition of sulphur and nitrogen. For the period 1979–2001 the trend in ozone, due to climate variability is increasing in central and southwestern Europe and decreasing in northeastern Europe, the trend in NO_2 is approximately opposite. The trend in PM is positive in eastern Europe. There are negative trends in wet deposition in southwestern and central Europe and positive trends in dry deposition overall. A bias in ERA40 precipitation could be partly responsible for the trends. The variation and trends need to be considered when interpreting measurements and designing measurement campaigns.

1. Introduction

Long-range transport, chemical and physical transformation and deposition of air pollutants are strongly dependent on meteorological conditions and vary considerably from year to year. Consideration of meteorological variability on different timescales, from hours to decades is, therefore, necessary when trying to understand trends in various air pollution components or when assessing and detecting the consequences of emission reductions aimed at improving air pollution levels.

Decreasing trends in emissions of sulphur dioxide (SO_2) and oxides of nitrogen (NO_x) and to some extent ammonia (NH_3) are reported from many parts of Europe, resulting in an improvement of the chemical composition of surface waters (Stoddard et al., 1999); however, biological recovery is not evident everywhere yet (Skjelkvåle et al., 2003). The total European emission decrease between the years 1980 and 2000 is 70% for SO_2, 30% for NO_x, 25% for NH_3 and 35% for non-methane volatile organic compounds (NMVOC; Lövblad et al., 2004; Grennfelt and Hov, 2005). The change in airborne concentrations of SO_2 (50–90% decrease) correspond to what is expected due to the emission reductions but the deposition has not decreased as much. One explanation is that the oxidation process is a relatively more important sink for SO_2 due to the emission reductions (Lövblad et al., 2004). The decrease in sulphate (SO_4^{2-}) in particulate matter (PM) has been between 50% and 75% depending on location, and corresponding for deposition; at most sites a correlation between SO_4^{2-} in air and precipitation exist. In Sweden, the total deposition has decreased by 75% during 1985–2000 (Lövblad et al., 2004). Another contributory cause to the trends in deposition of sulphur, which is investigated in this paper, could be a change in weather patterns. The picture is less clear for nitrogen; there are only a few long-term data series available. The decrease in total nitrate (NO_3^-) and total ammonium (NH_4^+) concentrations have been 20–30% in Denmark, Norway and the United Kingdom. Higher decreases (30–60%) in NO_3^- concentrations have been observed in Lithuania, the Slovak Republic and Sweden (Lövblad et al., 2004). Due to reductions in emissions of

*Corresponding author.
e-mail: Camilla.Andersson@smhi.se
DOI: 10.1111/j.1600-0889.2006.00196.x

NO_x and volatile organic compounds (VOC) there is a decrease in maximum tropospheric ozone (O_3) concentrations in Europe (Roemer et al., 2003; Solberg et al., 2005a; Jonson et al., 2006); however, the average background concentration at many remote stations (Ireland, Sweden, Finland, Norway, Scotland, mountain top sites) is unchanged or increasing (Solberg et al., 2005b): for example, Mace Head in Ireland has reported an increase of 0.5 ppbv yr^{-1} (Simmonds et al., 2004). This is probably due to a combination of effects including meteorological variability and increases in background tropospheric O_3 levels.

The aim of this study is to estimate the European interannual variability during 1958–2001 in concentrations of PM, O_3, nitrogen dioxide (NO_2), deposition of oxidized sulphur (SO_x-S) and reduced (NH_x-N) and oxidized nitrogen (NO_y-N) due to changes in meteorology, that is, omitting trends in emissions over the 44 yr. Another focus is to investigate if trends in O_3, NO_2, PM concentrations and deposition of SO_x-S, NH_x-N and NO_y-N exist due to changes in climate. We limit ourselves to the impact of meteorology and climate change in the lower troposphere of Europe, hence omitting changing climate outside the model domain giving rise to varying influxes across the model boundaries.

Earlier studies of this kind, using the previous ECMWF reanalysis, ERA15, for global scale chemistry transport model (CTM) simulations, have been presented by Lelieveld and Dentener (2000), focusing on the relative roles of chemistry and transport in global tropospheric ozone, and Peters et al. (2001), focusing on the El Niño-Southern oscillation signal in the simulated tropospheric O_3. Fusco and Logan (2003) presented an analysis of the trends in tropospheric ozone at northern mid-latitudes using the GEOS-CHEM model, covering the years 1970–1995. One conclusion of their study is that even though local increases in NO_x and the decrease in stratospheric ozone are the major factors affecting trends in tropospheric ozone, at least some of the spatial differences in the trends between North America and Europe may be due to differing temperature trends. In a preceding study (Andersson and Langner, accepted to the Acid Rain, 2005, Journal Special Issue of Focus: Water, Air and Soil Pollution) the interannual variability of O_3 and NO_2 were studied during 46 yrs (1958–2003) keeping the emissions constant.The study also showed low-frequency variations in O_3 and NO_2 due to variations in climate in the ERA40 analysis. In this study the issues of trends and interannual variation are pursued further. The present study brings new knowledge about the variation of concentrations of O_3, NO_2 and PM as well as the deposition of nitrogen and sulphur at present levels of emissions during a long time period, which may be valuable in making strategies for future emission reductions and interpretation of trends in measured air pollutants. The study also has implications for the design of measurement campaigns and environmental air quality surveillance, aiming at providing both temporally and spatially representative data and for Integrated Assessment Modelling assuming a limited number of years to be representative for a longer time period.

2. Methods

2.1. Chemical transport model

The Multi-scale Atmospheric Transport and Chemistry (MATCH) model was used in this study. MATCH is a three-dimensional, Eulerian model developed at the Swedish Meteorological and Hydrological Institute and it has been used earlier to simulate emission, transport, wet and dry deposition and chemical conversion on various scales, from urban (Gidhagen et al., 2005) to regional (e.g. Langner et al., 2005; Siniarovina and Engardt, 2005). The advection scheme is Bott-type (Bott 1989), using fourth-order scheme in the horizontal and a second-order scheme in the vertical. The mass consistent and shape preserving transport scheme is vital for this type of analysis where fractions and relative trends are derived; false signals due to numerical errors should be kept as small as possible. A complete description of the transport model can be found in Robertson et al. (1999) and a description of the gas-phase chemistry can be found in Langner et al. (1998). In this study the photochemistry scheme proposed by Simpson et al. (1993) is used with some modifications and updates; the most notable being a modified production mechanism for isoprene chemistry, based on the so-called Carter-1 scheme (Carter, 1996; Langner et al., 1998). The photochemical model includes about 130 reactions and 61 chemical components. The emission of isoprene is calculated using the E-94 isoprene emission methodology proposed by Simpson et al. (1995). The dry deposition of chemical species and aerosol is calculated using a resistance approach depending on land use. The wet scavenging is assumed to be proportional to the precipitation intensity for most gaseous components. For O_3, hydrogen peroxide (H_2O_2) and SO_2 in-cloud scavenging is calculated by assuming Henry's law equilibrium: subcloud scavenging is neglected for these species. All particulate sulphate inside clouds is assumed to be dissolved to cloud droplets; in-cloud scavenging is proportional to the fraction of the cloud water that hits the ground as precipitation. Subcloud scavenging for sulphate is calculated as in Berge (1993). The wet scavenging coefficients and dry deposition velocities at 1 m, for species with non-zero deposition, are given in Table 1. The wet scavenging coefficients for SO_2, O_3, H_2O_2, ammonium sulphate ($(NH_4)_2SO_4$) and SO_4^{2-} are non-zero, but depend on meteorology and are, therefore, indicated by a star sign in the table. For O_3 the dry deposition velocity over land is the same as above snow if the temperature is below 273 K.

Parametrized vertical transport due to convection was not included in the model runs in the present study. Earlier sensitivity studies with MATCH indicate that this is of small significance for the average surface concentrations of most

Table 1. Wet scavenging coefficients (Λ) and dry deposition velocities (v_d) for different land-use classes, sea and snow for species that are deposited. The intervals in dry deposition velocities indicate diurnal variation (the low value at night). Star(*) indicates wet scavenging by a more complex scheme (Berge, 1997).Units: Λ: h mm^{-1} s^{-1}, v_d: cm s^{-1}. x indicates that snow cover is not taken into account for dry deposition of the species.

Compound	Λ	v_d sea	v_d snow	v_d lowveg	v_d forest
O_3 (Nov–Feb)	*	0.05	0.05	0.3–0.45	0.3–0.45
O_3 (March)	*	0.05	0.05	0.3–0.45	0.3–0.6
O_3 (April)	*	0.05	0.05	0.3–0.7	0.3–0.6
O_3 (May)	*	0.05	0.05	0.3–0.7	0.3–0.7
O_3 (June, Aug–Oct)	*	0.05	0.05	0.3–0.7	0.3–0.8
O_3 (July)	*	0.05	0.05	0.3–0.8	0.3–0.8
H_2O_2	*	0.6	x	1	1
SO_2 (Nov–May)	*	0.5	0.06	0.3–0.8	0.6–1.3
SO_2 (June)	*	0.5	0.06	0.3–0.8	0.7–1.5
SO_2 (July)	*	0.5	0.06	0.3–0.8	1–1.7
SO_2 (Aug–Sep)	*	0.5	0.06	0.3–0.8	1–1.8
SO_2 (Oct)	*	0.5	0.06	0.3–0.8	0.7–1.4
SO_4^{2-}	*	0.05	x	0.1	0.5
$(NH_4)_2SO_4$	*	0.05	x	0.1	0.5
NO_3	3.89E−04	0.5	x	2	2
NH_3 (Nov–Mar)	3.89E−04	0.6	0.2	2	2
NH_3 (Apr–May)	3.89E−04	0.6	0.4	1.5	1.5
NH_3 (Jun–Aug)	3.89E−04	0.6	0.4	1	1
NH_3 (Sep)	3.89E−04	0.6	0.4	1.2	1.2
NH_3 (Oct)	3.89E−04	0.6	0.2	1.5	1.5
N_2O_5	3.89E−04	0.5	x	2	2
NH_4NO_3	2.78E−04	0.05	x	0.1	0.5
NO_3^-	2.78E−04	0.05	x	0.1	0.1
HNO_3 (Dec–Feb)	3.89E−04	1	x	4	4
HNO_3 (Mar–Nov)	3.89E−04	1	x	4	5
HCHO	1.40E−05	0.2	x	0.2	0.2
C_2H_5OH	3.89E−04	0.5	x	0.1–0.6	0.1–0.6
CH_3OH	3.89E−04	0.5	x	0.1–0.6	0.1–0.6
HO_2	3.89E−04	0.6	x	0.6	0.6
O	3.89E−04	0.5	x	2	2
OH	3.89E−04	0.7	x	0.7	0.7
NO_2	0	0	0.1	0.1–0.4	0.2–0.6
CH_3CHO	0	0.1	x	0.1	0.1
$CH_3COC_2H_5$	0	0.1	x	0.1	0.1
CH_3O_2	0	1	x	1	1
CH_3O_2H	0	0.1	x	0.1	0.1
C_2H_5OOH	0	0.1	x	0.1	0.1
ISOPROD	0	0.1	0.1	0.1	0.1
GLYOX	0	0	x	0.1	0.1
MGLYOX	0	0.3	x	0.05	0.05
$OXYO_2H$	0	0.1	x	0.1	0.1
$SECC_4H_9O_2H$	0	0.1	x	0.1	0.1
$MALO_2H$	0	0.1	x	0.1	0.1
ONIT	0	0.1	x	0.1	0.1
PAN	0	0	x	0.05–0.25	0.05–0.25

pollutants in a regional model study like this. Ozone, however, is probably an exception and will systematically be increased near the surface with convective transport turned on.

Emissions of sea salt (SS) were calculated using the method described by Foltescu et al. (2005) based on methodologies proposed by Mårtensson et al. (2003) and Monahan et al. (1986). The number of size bins can be varied, in this study SS and

Table 2. Budget of ozone, sulphur, reduced and oxidized nitrogen. The turnover time for ozone exclude chemical destruction. Unit: mass in model domain: Gg, fluxes: Gg yr^{-1}, turnover time: days.

	O_3	Oxidized N	Reduced N	Oxidized S
Mass in model domain	7.62×10^3	4.39×10^1	1.41×10^1	4.67×10^1
Emission	–	5.67×10^3	4.55×10^3	9.91×10^3
Inflow	1.10×10^6	4.02×10^3	1.17×10^3	2.54×10^3
Outflow	1.08×10^6	3.88×10^3	8.93×10^2	3.00×10^3
Dry dep	6.51×10^4	1.83×10^3	1.93×10^3	2.94×10^3
Wet dep	4.67×10^{-1}	4.00×10^3	2.91×10^3	6.54×10^3
Sum of losses	1.14×10^6	9.70×10^3	5.73×10^3	1.25×10^4
Turnover time	2.43	1.65	8.95×10^{-1}	1.37
Turnover time excluding outflow	4.27×10^1	2.75	1.06	1.80
Net chemical production	4.19×10^4	–	–	–

primary PM (PPM) were both divided into four bins[1]. No physical or chemical processes were considered except for emission, transport, wet and dry deposition of the PM and formation of secondary inorganic aerosol (SIA; SO_4^{2-}, NO_3^- and NH_4^+), hence there was no transformation between size bins. The concentrations of SS and PPM were calculated separately from the photochemistry. Wet scavenging coefficients for SS and PPM were determined on-line, using the monodisperse washout coefficient formulation in Dana and Hales (1976). In this study hygroscopic growth was taken into account for both SS and PPM in the calculation of dry deposition. A growth function, specified for sulphurous particles, by Koutrakis et al. (1989)and modified by Quinn and Ondov (1998) was used. The dry deposition of SS and PPM was calculated using the method formulated by Zhang et al. (2001).

Budgets for O_3, sulphur, oxidized and reduced nitrogen for 1999 can be found in Table 2, giving an estimation of the approximate lifetime of sulphur and nitrogen in the model domain. The high values for transport of O_3 are due to relatively high background concentrations of ozone in the free troposphere. The difference between sources and losses for O_3 indicate the net chemical production during 1999. Presently it is not possible to calculate the turnover time for O_3: in Table 2 the lifetime due to physical processes (deposition and out flux) is stated.

2.2. *Emission data and boundary conditions of chemical compounds and PM*

Input to the model comprised emissions, land-use, boundary conditions and driving meteorological data. Sector-divided emissions, for simulation of SIA, O_3 and NO_2, were derived from the 50 km resolution EMEP expert emissions (Vestreng, 2003) of NO_x, oxides of sulphur (SO_x), carbon monoxide (CO), NMVOC and NH_3. Sector divided emissions of anthropogenic primary emitted PM were derived from the 50 km resolution emission files provided by the EuroDelta project (Internet URL: http://rea.ei.jrc.it/netshare/thunis/eurodelta/, January 2005). These are re-gridded emissions, based on 50 km resolution emissions produced by EMEP. The emissions of the year 2000 were used throughout the entire simulation, except for isoprene and SS, which were calculated on-line.

Boundary concentrations were based on data from earlier MATCH model projects (e.g. Solberg et al., 2002, 2005a; Tilmes et al., 2002; Näs et al., 2003; Roemer et al., 2003). Monthly or seasonally varying lateral boundary conditions were used for some species. The boundary conditions are partly based on observations at background locations and partly on large-scale model calculations. For most species a value, c_i, was assigned for each boundary (c_{north}, c_{east}, c_{west}, c_{south} and c_{top}), where c_{top} specifies the value at the top surface and the other specify the ground level concentration in the middle of the sides. Linear interpolation is used between the points on the sides. The lateral O_3 boundary concentrations are based on back-trajectory analysed measurement data for 1999 from EMEP measurement stations (Internet URL: http://www.emep.int) and the top concentrations on sonde data from Ireland, the United Kingdom and Norway (average for the year 1996–2001). Other species with monthly or seasonally varying values are SO_2, methane (CH_4), VOC, SO_4^{2-}, peroxyacetyl nitrate (PAN), NO_3^-, ammonium nitrate (NH_4NO_3) and $(NH_4)_2SO_4$. The boundary values are given in the Appendix. For PPM and SS the boundary values were set to zero. Initial conditions were interpolated from the specified lateral boundary values.

This study does not aim to explain the interannual variability and trends in air pollution over Europe due to variability and climate change in the area outside the model domain. There are factors in the global climate and variability that could affect European air pollution other than the European meteorology investigated in this study; for example changes in import of air pollution across the lateral boundaries due to changing wind patterns or changes in the budgets of air pollutants outside the model domain due to changes in meteorology and climate. Also, the description of stratosphere–troposphere transport is

[1]Dry radius intervals of bins one to four are: 0.01–0.05 μm, 0.05–0.5 μm, 0.5–1.25 μm and 1.25–5 μm.

simplified due to the fact that the top boundary in this study is set in the middle of the troposphere. O_3 can be transported from higher concentrations aloft by descending air. The variability resulting from such transport is only crudely accounted for in the present study and should be investigated further in future studies.

2.3. Meteorological input data

2.3.1. ERA40. The basis for this study is the use of meteorological data from the recent global meteorological reanalysis ERA40 performed at the European Centre of Medium-range Weather Forecasts (ECMWF) (Uppala et al., 2004, 2005). Atmospheric data assimilation comprises a sequence of analysis steps in which background information for a short period, typically 6 hr, is combined with observations for the period to produce an estimate of the state of the atmosphere, the analysis, at a particular time. The background information comes from a short-range forecast initiated from the most recent preceding analysis in the sequence. Problems for climate studies arise partly because the atmospheric models used to produce these 'background forecasts' are prone to biases. If observations are abundant and unbiased, they can correct the biases in the background forecasts when assimilated. In reality, however, observational coverage varies over time, observations are themselves prone to bias, both due to instrumental- and spatial non-representativity and these observational biases can change over time. This introduces trends and low-frequency variations in analyses that are mixed with the true climatic signals. Awareness of how these factors influence the sequence of analyses is of great importance when using the reanalysis data as input to a CTM since the atmospheric chemistry and long-range transport and deposition of air pollutants are closely coupled to various aspects of meteorological processes. Transport patterns are linked to the distribution of atmospheric wind systems on different scales. Atmospheric chemistry is linked to temperature, radiation, humidity and presence of clouds. Deposition processes are linked to the distribution and amount of precipitation and clouds as well as to the turbulence structures of the atmospheric boundary layer.

Based on the observational data used in ERA40, the time period 1958–2001 can be divided into three parts: the satellite period 1989–2001 with a large amount of satellite data assimilated into the ERA40 system, the pre-satellite period 1958–1972 with no satellite data available, and the transition period 1972–1988 where the amount of satellite data assimilated increases over the period. The ERA40 reanalysis has several known deficiencies linked to the use of different data sources that has limited the usefulness of the data set for *global* CTM studies. Two of the most serious problems in ERA40 products are a too strong Brewer-Dobson circulation in the stratosphere and excessive tropical oceanic precipitation in short-range forecasts run from the analyses (Uppala et al., 2005). The latter affects the analysis of humidity, while the outwash decreases the humidity. Further (but smaller) deficiencies in the assimilating model include (Uppala et al., 2005) uncorrected radiosonde temperatures prior to the year 1979. Specific humidity measurements were also known to suffer from biases, which were not corrected. There was no inclusion of trends or temporal variation in aerosol in ERA40 and there was no variation in the land-use characteristics. Due to an error in the conversion of humidity measurements in one of the early sets of radiosonde data the specific humidity in the tropics is especially poor from early 1958 to early 1963 (Uppala et al., 2005). This caused widespread mean drying increments and lower precipitation, which is seen in for example hydrological studies for North America (Hagemann et al., 2005). A comparison between a short-range forecast and model independent data of vertically integrated water vapour (IWV), the dominant contribution being boundary layer moisture, shows a bias of 2% globally (Andersson et al., 2005). For the whole globe, the trend for the period 1979–2001 in IWV is probably an artefact of changes in observing system: it is twice as large as the trend determined from the Clausius-Clapeyron relation assuming conservation of relative humidity (Bengtsson et al., 2004). There is a general improvement in surface pressure and temperature analyses at 500 hPa over the period of ERA40. In the end of 1978 there was a major improvement of the overall observing system. The effect of this is especially obvious in the southern hemisphere.

For the extra-tropical Northern hemisphere the basic synoptic quality of ERA40 was tested by comparing synoptic maps from the ERA40 analyses and forecasts to published contemporary analyses (Uppala et al., 2005). For the whole period the percentage detection rate of tropical cyclones was above 90% throughout the period in the Northern hemisphere when comparing ERA40 to an independent best-track data set (Uppala et al., 2005).

In this study we use the results from ERA40 in a regional CTM study over the European domain. This area has a quite good coverage of observational data compared to the tropical regions of the globe and the analysis can, therefore, be expected to be better constrained by observations in this region. For humidity this is indicated by small differences, less than 2%, between analysis and 1 d forecasts of zonal average relative humidity in the northern hemisphere mid-latitudes. The corresponding differences in the tropics are larger but generally less than 5% (Andersson et al., 2005). Simmons et al. (2004) have compared monthly mean surface air temperature from ERA40 and corresponding data derived directly from monthly station data (CRUTEM2v). Their study reveals mostly similar short-term variability in surface temperatures with a 99.6% correlation for the European domain for the period 1958–2001. The trend for Europe in ERA40 is about 30% weaker compared to CRUTEM2v for the period 1958–2001 (0.11 °C per decade) while the trend for 1979–2001 is within 10% (0.42 °C per decade). The good performance of ERA40 in comparison with CRUTEM2v is partly due to specific analysis of the 2 m temperature in ERA40. Trends in ERA40 are weaker if 2 m temperature derived directly from the variational analysis

is compared to CRUTEM2v. The trends in this case are about 60% weaker for the 1958–2001 period (0.06 °C per decade) but less than 20% weaker for the 1979–2001 period (0.37 °C per decade). The short-term variability is still similar with a 99.1% correlation for Europe between ERA40 and CRUTEM2v for the period 1958–2001. The two step changes in the analysis system in 1972 and 1988/1989, cased by changes in the amount of data and changes in the assimilation associated with correction of biases in the data only show by a few signs; small jumps in the mean temperatures in the troposphere due to differences in satellite bias corrections and larger jumps in the stratospheric mean temperature (Uppala et al., 2005).

The work by Hagemann et al. (2005) shows that the ERA40 hydrological cycle over Europe has improved compared to the previous ERA15 reanalysis (Kållberg, 1997), specifically over land the improvements comprise eliminated cold biases in winter, reduced occurrence of negative P-E (precipitation minus evapotranspiration) values, removed dry bias in winter, and an improved representation of the snow pack. Comparison with GPCP (Global Precipitation Climatology Project; Huffman et al., 1997) data over Europe indicates quite good agreement between ERA40 and land-based observations of precipitation. The correlation for monthly precipitation for European land points for the period 1979–2001 is 92.4% and the fractional bias −27%. For Scandinavia the corresponding statistics are 95.6% and −23% (personal communication with Per Kållberg at the Swedish Meteorological and Hydrological Institute 2005). However, further comparisons between GPCP and ERA40 indicate that the agreement in trends in precipitation over Europe is not as good. Comparison of trends in annual average precipitation over European land points showed that the trend in the ERA40 data is 40% stronger than the one in GPCP (−3.7% versus −2.7% per decade). Trends and statistics were also calculated for six subareas of Europe. There are substantial differences between the ERA40 and GPCP trends over both the southeastern (2.4% and −5.2% per decade) and southwestern (−6.6% and 1.6% per decade) European land areas, the correlation also being fairly low for annual averages down to 0.75 for southwestern Europe. For northern Europe the trends agree much better. Over central Europe the negative trend is about twice as strong in the ERA40 data set as in GPCP. The average total precipitation is underestimated by 18–34% in ERA40 compared to GPCP, and for fractional standard deviation the difference in ERA40 compared to GPCP is −7% to +25%, the largest difference occurs in central Europe. Hagemann et al. (2005) also shows that the difference between ERA40 and observations has decreased (ERA40 underestimating in all three periods) in the Danube catchment (southeastern Europe) during the three time periods and in the Baltic catchment (parts of northern Scandinavia and northeastern Europe) the error has been small, but changing between overestimations (1973–1988) and underestimations.

The tendency for underestimation of precipitation in ERA40 is likely to affect the modelled budgets of air pollutants over Europe. Residence times and transport distances of soluble chemical components can be expected to be somewhat overestimated. As can be seen in the validation section, the wet deposition of nitrate and ammonium are underestimated by about 16% (for the year 1999). Also the difference in trends between GPCP and ERA40 could introduce trends in the simulated data, which are not due to actual climate variability. In conclusion, great care needs to be taken when analysing trends in air pollutants over Europe using the ERA40 data set.

2.3.2. The use of ERA40 in MATCH. In this study 6 hourly meteorological data of the lowest 21 levels, spanning from 10 m to 5 km, from the ERA40 meteorological data set were used, except for the calculation of a balanced three-dimensional wind field, for which the lowest 39 levels were used. All data were taken from analyses except precipitation and albedo, which were taken from the 6 hr forecast. The ERA40 data were interpolated from the original 125 × 125 km horizontal resolution to 0.4° × 0.4° (*ca*. 44 km) used by MATCH to take advantage of the 50 km emission data resolution, and in time to 1 hr data. The 21 vertical levels in ERA40 also define the vertical levels in MATCH. The ERA40 meteorological data set stretches from September 1957 to August 2002. In this study it was used to run the model from 1958 to 2001.

Most meteorological parameters described in this paragraph are used in many parts of the code: here we give the main applications. Horizontal winds (U, V) at model levels were used for calculation of horizontal and vertical advection and boundary layer processes, such as turbulent vertical mixing and dry deposition of chemical species and aerosol, as well as calculating emissions of SS (lowest level wind). Horizontal diffusion is neglected under assumption that it is small compared to the advection with the horizontal wind. For calculation of vertical wind, the horizontal wind at the lowest 39 levels (reaching 49 mbar) and the tendency of surface pressure (LNSP) were used. Temperature (T) at model levels is used for calculation of boundary layer processes, temperature-dependent chemical transformations and photolysis, and emissions of SS and biogenic emissions (isoprene). Precipitation (TP; sum of large scale precipitation and convective precipitation, including snow fall), total cloud water content (CWC; sum of cloud ice water content and cloud liquid water content) at model levels are used for calculating wet deposition and the cloud liquid water content is also used in aqueous phase sulphur chemistry, involving O_3, SO_4^{2-}, $(NH_4)_2SO_4$ and SO_2. Precipitation is also used in estimation of the cloud transmittance for global radiation for photolysis rates and emissions of isoprene. Snowdepth (SD) is used as an indication of snow cover, which is used in the calculation of dry deposition of ozone, boundary layer processes, and for calculation of global radiation. Cloud cover (CC) at model levels and total cloud cover (TCC; including specification of high, middle and low clouds) are used for calculations of global radiation. Specific humidity (Q) at model levels is used for calculation of boundary layer processes and dry deposition of PPM and SS. Other parameters used

Table 3. Average (unit: $\mu g/m^3$), fractional bias (unit: %) and correlation of measured (OBS) and simulated (MATCH) daily PM_{10} and $PM_{2.5}$ concentration during 1999. Only stations with more than 122 (33%) measurements are displayed. Sites are coded in the system of EMEP (http://www.emep.int).

	PM10					PM2.5				
	OBS Mean	MATCH Mean	Bias	Corr	#meas	OBS Mean	MATCH Mean	Bias	Corr	#meas
Global	14.43	6.40	−55.63	0.56	5079	11.36	5.22	−54.01	0.56	1676
CH02	20.59	6.37	−69.05	0.59	341	15.88	5.99	−62.31	0.53	347
CH03	18.79	5.57	−70.37	0.53	355	–	–	–	–	–
CH04	12.88	6.88	−46.58	0.62	315	8.69	6.52	−24.95	0.64	341
CH05	11.79	6.08	−48.38	0.58	360	–	–	–	–	–
DE01	19.72	5.91	−70.04	0.70	348	–	–	–	–	–
DE02	16.46	7.95	−51.69	0.71	343	11.87	7.77	−34.52	0.66	278
DE03	8.13	7.09	−12.80	0.58	349	–	–	–	–	–
DE04	14.42	8.54	−40.77	0.73	356	–	–	–	–	–
DE05	10.54	8.48	−19.53	0.60	364	–	–	–	–	–
DE07	14.57	6.85	−53.00	0.62	364	–	–	–	–	–
DE08	12.51	7.88	−37.06	0.73	364	–	–	–	–	–
DE09	17.02	6.91	−59.40	0.61	363	–	–	–	–	–
SE12	12.58	2.63	−79.05	0.63	263	9.81	2.53	−74.19	0.60	273
SE41	12.24	3.66	−70.06	0.75	134	11.16	3.54	−68.23	0.75	136
SE42	13.49	4.58	−66.09	0.62	162	10.51	4.75	−54.80	0.65	151
SE44	13.58	2.77	−79.62	0.64	298	9.87	2.69	−72.76	0.65	150

are surface temperature (TS) for boundary layer processes, and forecast albedo (FAL), which is used in calculations of global radiation.

3. Comparison with observed concentrations and deposition for 1999

The MATCH model has recently been compared to observations, and also to other European scale CTMs, for the year 1999 and 2000 as part of the assessment of the EMEP Unified model (van Loon et al., 2004) showing good performance compared to other models. However, in that study a different meteorological driver was used for MATCH; the High Resolution Limited Area Model (HIRLAM) run operationally at SMHI and providing meteorological fields at a 44 × 44 km resolution. Here we use ERA40 that has a coarser horizontal and different vertical resolution; hence a new assessment of the model performance is needed.

Table 3 shows a comparison between observed and simulated hourly O_3, daily SO_2, NO_2, SO_4^{2-}, NO_3^-, nitrous acid (HNO_3), NH_4^+ and NH_3 as well as wet deposition of SO_4^{2-}, NO_3^- and NH_4^+ at EMEP stations (EMEP/CCC, 1999; Hjellbrekke, 2001). Table 4 shows a comparison between simulated (first level, ca. 10 m.) and observed PM at background locations. To validate modelled PM, where simulated SIA and the first two bins of SS and PPM represents modelled PM with a diameter less than 2.5 μm ($PM_{2.5}$), since the diameter refers to wet particles and calculations (based on Gong et al., 1997; not shown) on hygroscopic growth in SIA and SS shows that the diameter in bin two grows by approximately 17–33% and 25–47%, respectively (on average in June 2002), depending on location. Other studies, for example Svenningsson et al. (1994), support these numbers. Some even indicate higher diameter growth factors (e.g. Swietlicki et al., 1999, 2000). SIA and all four bins of SS and PPM represents modelled PM with a diameter less than 10 μm (PM_{10}). A comparison was conducted to measured daily concentrations of $PM_{2.5}$ and PM_{10}, retrieved from the EMEP homepage (EMEP/CCC, 1999; Hjellbrekke, 2001).

The concentrations of modelled and measured O_3 show good agreement, the daily maximum of hourly average concentrations displaying better correlation than the daily average concentrations. The O_3 average and maximum concentrations are underestimated by 10%, at least part of the underestimation is due to too small downward transport of free tropospheric O_3 to the surface levels. Contrary to all other airborne concentrations the spatial correlation (the correlation of measured and simulated temporal average at the sites) of O_3 is lower than the global correlation. The daily average spatial correlation is only 0.46, which is indicating that the underestimation is not smoothly distributed over the model area. For the other airborne concentrations the global correlation is lower than for O_3, and the bias vary between −17% and +29%. The lowest correlation we see for SO_4^{2-}-part, 0.29, and the highest correlation we find for sodium (Na^+), 0.59. Generally the nitrogen containing compounds show higher correlation between the modelled and measured concentrations than the sulphur containing compounds and the bias is also generally smaller.

Table 4. Observed (OBS) and calculated (MATCH) mean, fractional bias and correlation for the year 1999 of hourly mean or daily max O_3, daily concentrations of air pollution or monthly accumulated wet deposition. All available EMEP measurement stations were included in the evaluation of O_3, except two stations: SI31 and SI33 (Kovac, 2002). For O_3 and Na^+ the global correlation stated is the mean of the correlation coefficients at each site, weighted with the number of paired values. Units: average: O_3: ppbv; other conc.: μg (S/N) m^{-3}; wet dep.: mg (S/N) m^{-2}; fractional bias: %.

	Global					Spatial				
	OBS Mean	MATCH Mean	%bias	Corr	#cases	OBS Mean	MATCH Mean	%bias	Corr	#cases
O_3 mean (h)	32.29	29.19	−9.6	0.59	842706	32.62	29.30	−10.2	0.46	106
O_3 max (d)	42.70	37.93	−11.2	0.72	36059	43.05	38.10	−11.5	0.63	106
Na^+	0.59	0.65	9.5	0.59	7458	0.70	0.67	−4.4	0.53	8
SO_2	0.94	1.21	28.5	0.35	29537	0.95	1.32	39.5	0.51	88
SO_4^{2-}	0.76	0.70	−8.1	0.294	26365	0.77	0.71	−7.8	0.73	82
NO_2	2.07	1.86	−10.1	0.485	22688	2.11	2.06	−2.4	0.61	68
NO_3^-	0.51	0.48	−5.1	0.503	6725	0.49	0.47	−4.0	0.87	20
$HNO_3+NO_3^-$	0.45	0.45	0.3	0.393	13424	0.46	0.46	0.3	0.75	40
NH_4^+	0.87	1.00	14.3	0.443	8149	0.84	0.96	14.4	0.71	25
$NH_3+NH_4^+$	1.23	1.12	−9.2	0.55	13656	1.25	1.13	−9.3	0.72	41
SO_4-wet	40.54	40.20	−0.8	0.401	905	40.49	39.97	−1.3	0.57	78
NO_3-wet	27.44	23.01	−16.2	0.37	905	27.04	23.03	−14.8	0.56	78
NH_4-wet	30.06	25.03	−16.7	0.296	905	29.77	25.07	−15.8	0.47	78

The particulate NO_3^- and NH_4^+ are overestimated overall, while particulate SO_4^{2-} is underestimated. For all sites total PM is underestimated, which is expected since the modelled PM only contains SIA, SS and PPM, omitting for example natural mineral dust and secondary organic aerosol. Another missing component in the PM is water. With increasing relative humidity the aerosol particles grow hygroscopically; however, the measurement method used should remove water from the particles and hence the missing mass cannot be explained by water. Hygroscopic growth is taken into account within MATCH for calculation of the deposition velocity of PPM and SS. However, in MATCH all PM concentrations are stored as dry mass concentrations. The dry PM_{10} and $PM_{2.5}$ from the EMEP aerosol model have also been compared to measurements for the years 1999–2001. The model was found to underestimate the concentrations by 40–60% on average (Tsyro, 2005). In this comparison MATCH underestimates the concentrations by 10–80% depending on location, with the smallest underestimation at the German sites.

The bias for wet deposition of sulphur and nitrogen is low; however, the correlation is low as well. One reason for this could be that the location and amount of precipitation as predicted by the ERA40 6 hr forecast are not as accurate as the model needs for calculating wet deposition. Also the horizontal resolution in the original ERA40 fields is rather low compared to the regional scale meteorological data from HIRLAM that has been used previously, hence it is expected that the model does not perform as well as in previous studies. However, all current European-scale models trying to simulate wet deposition of chemical compounds have difficulties (van Loon et al., 2004).

It is apparent that the simulated concentrations and deposition show fairly good agreement with measurements for 1999. In conclusion we believe that the model performance and present model set-up is good enough for studies of the impact of meteorological variability on air pollution over the period 1958–2001.

4. Results and discussion

4.1. Interannual variability of concentrations and deposition

In Fig. 1 the annual deviation of $PM_{2.5}$ from the 1958–2001 average is displayed. The deviation varies between −50% and 100% for larger areas; however, the average of the fractional standard deviation (fsd) is only 9.1% over land areas which can be seen in Table 5. A clear low-frequency variation can be seen: during the first 10 yr the average deviation is positive, becoming negative in the next 13 yr and thereafter becoming positive again. The deviations of summer O_3 and annual NO_2 are published elsewhere (Andersson and Langner, accepted to the Acid Rain, 2005, Journal Special Issue of Focus: Water, Air and Soil Pollution). Figure 2 shows the 44 yr (1958–2001) average and fsd of summer O_3 (average over April to September) and annual NO_2, $PM_{2.5}$, $PPM_{2.5}$, SIA and $SS_{2.5}$. The largest fsd generally occurs where the average concentration is low for the constituents of PM, such as over land for $SS_{2.5}$ and over the Atlantic for $PPM_{2.5}$. The absolute standard deviation is generally highest where the concentration is high, but never reaching the value of the 44 yr average. The variation of PM over sea is mainly governed by the variation in SS. Over land the variation is governed by both

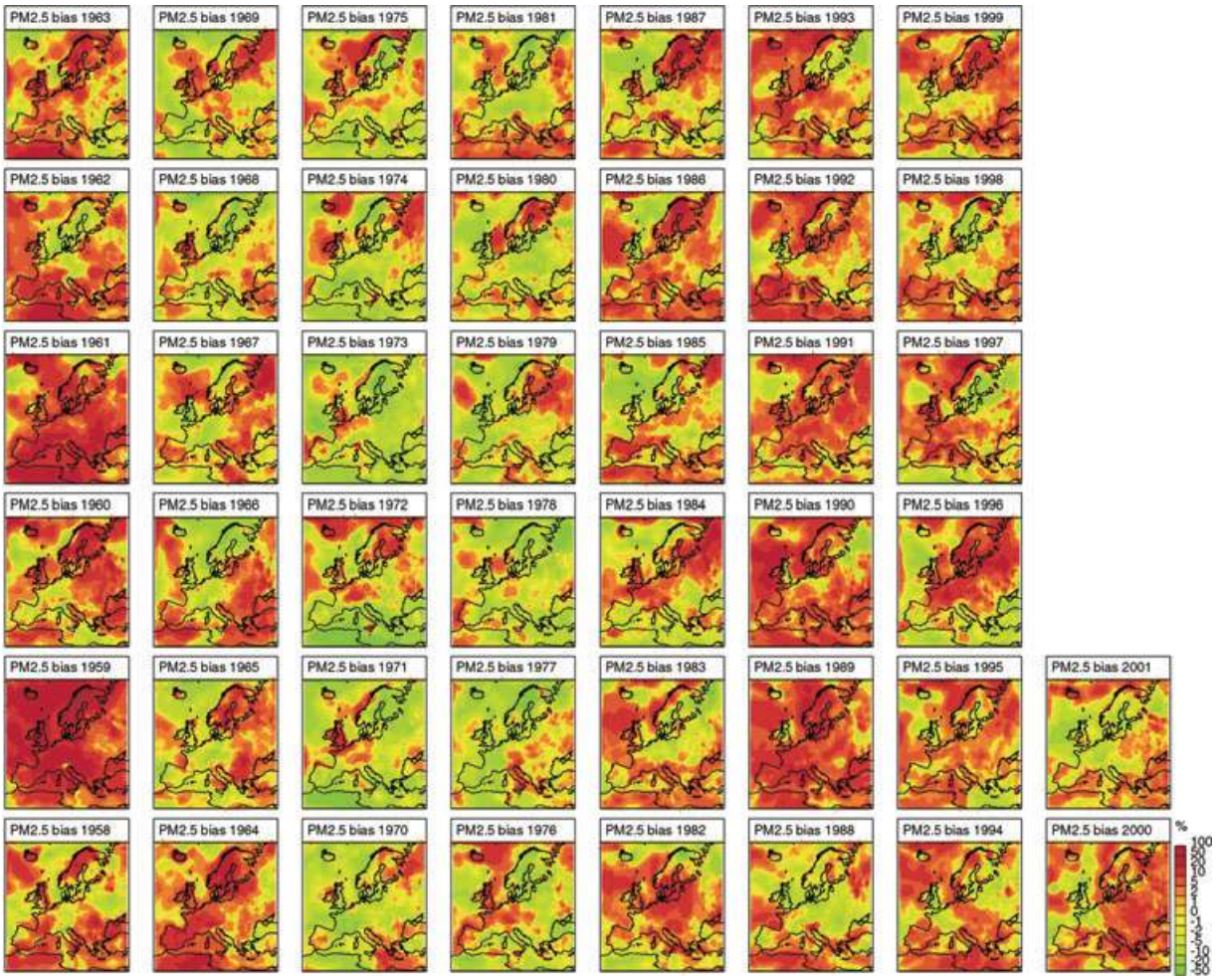

Fig. 1. Fractional bias (unit: %) of annual mean $PM_{2.5}$ concentration compared to the 44 yr average (1958–2001). The fractional bias is defined as $\frac{M_{\text{year}} - M_{\text{all years}}}{M_{\text{all years}}} \cdot 100$

the variation in SIA and $PPM_{2.5}$, with SIA being slightly more dominant away from large sources of PPM. This is an effect of the magnitude of the concentrations, where the SS is the largest component of PM over sea and SIA mostly the largest over land. Since part of PM is missing, as discussed earlier, the interannual variability in $PM_{2.5}$ due to meteorological variability shown in Fig. 1 should be interpreted with caution. The variation in SIA and especially $PPM_{2.5}$ is often higher than for $PM_{2.5}$. The variation of PM_{10} is very similar to that of $PM_{2.5}$, the difference being slightly higher deviation in PM_{10} than in $PM_{2.5}$.

Table 5 shows averages over regions for the 44 yr as well as geographically averaged fsd, maximum positive fractional deviation (maximum over the years of the annual fractional bias for each grid point) and minimum negative fractional deviation (minimum of the negative fractional bias for each grid point). In Fig. 3 the six subareas of land, referred to in Table 5, are displayed. The average European land-area fsd ranges from 3% for O_3, 5% for NO_2, 9% for PM and primary PM, 6–9% for dry deposition of SO_x-S, NH_x-N and NO_y-N, 11% for secondary inorganic aerosol, 11–14% for total deposition of SO_x-S, NH_x-N and NO_y-N to about 20% for wet deposition of SO_x-S, NH_x-N and NO_y-N and SS concentrations. A comparison between the variability in SIA (8–18% depending on location) and the decrease in SO_4^{2-} in particles (2.5–3.8% per year; Lövblad et al., 2004) and NO_3^-/NH_4^+ in particles (1–3% per year; Lövblad et al., 2004) shows that the fsd on the average is greater than the decrease due to emission reductions.

For five chosen meteorological parameters, at first or surface level, geographically averaged 44 yr averages, fsd, maximum positive and minimum negative deviations are displayed in Table 6. We see that precipitation displays the greatest fractional standard deviation and maximum fractional deviation, whereas temperature displays the lowest variation. This agrees with the wet deposition displaying the greatest, and ozone and NO_2 displaying the lowest average interannual variability, since these are governed more by factors such as temperature, humidity, radiation and stability. We also see that the geographically averaged maximum deviation is greater than the minimum deviation

Table 5. Top section: Regional average concentration and deposition for the period 1958–2001. Top middle section: Regional averages of fractional standard deviation (fsd). Bottom middle section: Regional averages of maximum fractional deviation. Bottom section: Regional averages of minimum fractional deviation. Index d means dry deposition, w wet deposition and t total (=wet + dry) deposition. Units: average: O_3, NO_2: ppb(v), PM_{10}, $PM_{2.5}$, $PPM_{2.5}$, $SS_{2.5}$, SIA: $\mu g\ m^{-3}$, SO_xSd, SO_xSw, SO_xSt, NO_yNd, NO_yNw, NO_yNt, NH_xNd, NH_xNw and NH_xNt: $mg\ m^{-2}$; fsd and fractional deviation: % of 44 yr average.

	O_3	NO_2	PM_{10}	$PM_{2.5}$	$PPM_{2.5}$	$SS_{2.5}$	SIA	SO_xSd	SO_xSw	SO_xSt	NO_yNd	NO_yNw	NO_yNt	NH_xNd	NH_xNw	NH_xNt	
Overall	36.37	1.56	9.67	7.24	1.25	2.18	3.81	169	352	521	103	216	318	112	157	268	
Land	31.40	1.94	8.09	6.76	2.01	0.40	4.35	186	424	611	140	226	366	190	213	402	
Sea	41.50	1.17	11.30	7.75	0.47	4.02	3.26	152	276	428	64	205	269	31	99	130	
GB-IR-IC	32.75	3.39	8.58	6.48	1.24	1.88	3.36	158	306	464	162	227	389	218	209	427	Geographical average of average concentration and deposition for 1958—2001
Scandinavia	31.46	1.22	3.59	2.89	0.77	0.56	1.56	63	251	315	86	213	298	62	133	195	
NE Eur	30.18	1.00	6.56	4.84	2.25	0.12	2.48	127	411	539	93	205	298	106	187	293	
SW Eur	34.28	3.00	9.64	8.56	2.12	0.69	5.74	151	346	498	205	230	434	340	242	581	
SC Eur	35.50	4.56	12.73	11.28	3.17	0.43	7.68	372	589	962	283	396	679	402	393	795	
SE Eur	32.88	1.56	10.76	9.36	2.40	0.23	6.74	331	714	1045	136	219	355	199	223	422	
Overall	2.7	6.4	8.6	8.8	14.5	15.7	13.6	8.5	17.8	13.1	9.0	17.0	11.3	15.2	19.8	14.9	
Land	3.1	5.1	8.8	9.1	9.2	20.3	11.3	8.9	18.8	13.9	6.3	18.5	11.0	7.8	19.4	11.9	
Sea	2.3	7.7	8.4	8.5	19.9	11.1	16.0	8.0	16.7	12.3	11.7	15.5	11.5	22.9	20.2	17.9	
GB-IR-IC	3.0	10.0	9.2	10.3	12.6	12.6	17.7	10.1	15.7	12.5	10.6	16.2	11.5	7.5	16.3	10.9	
Scandinavia	3.5	6.4	12.9	12.5	9.8	23.3	18.3	12.8	16.4	14.7	7.8	13.6	10.6	12.2	17.1	14.1	Geographical average of fractional standard deviation for 1958–2001
NE Eur	3.1	5.4	8.3	8.6	9.3	25.3	10.4	9.3	12.4	10.2	6.4	11.6	8.6	9.9	13.4	10.1	
SW Eur	2.8	4.1	8.0	8.5	6.7	14.6	10.7	6.9	21.2	14.3	5.3	22.1	10.4	4.4	23.0	8.7	
SC Eur	3.3	4.0	7.5	7.9	6.6	18.6	9.6	6.9	16.7	11.8	4.3	15.5	8.6	5.0	15.7	7.9	
SE Eur	2.3	4.0	6.9	7.2	6.2	18.9	8.3	6.6	17.4	12.3	4.8	17.7	10.5	5.1	17.9	9.5	
Overall	5.9	15.1	22.4	23.7	37.3	39.9	40.3	20.7	46.1	33.8	22.2	42.6	27.8	41.2	51.3	39.0	
Land	6.7	11.4	23.8	24.9	22.6	52.6	31.5	21.7	48.6	35.6	15.3	47.1	27.4	19.4	49.7	30.9	
Sea	5.0	18.8	20.8	22.4	52.5	26.7	49.3	19.6	43.6	31.9	29.3	38.0	28.2	63.7	53.0	47.4	
GB-IR-IC	6.9	21.8	29.7	35.0	32.1	34.6	59.3	25.4	36.8	29.8	28.9	36.0	25.8	18.9	40.0	28.7	Geographical average of maximum positive fractional deviation for 1958–2001
Scandinavia	7.4	15.6	42.7	44.3	24.7	64.6	68.8	35.1	45.0	40.3	23.6	33.3	26.3	36.5	43.1	35.8	
NE Eur	6.7	12.0	20.7	20.9	23.3	69.1	24.6	23.9	28.6	23.5	15.4	26.2	19.2	24.3	31.5	23.5	
SW Eur	6.6	9.5	20.4	21.6	15.2	35.1	26.9	16.1	49.8	33.0	12.6	50.7	23.3	10.3	53.7	20.9	
SC Eur	6.8	8.8	22.1	23.3	16.1	47.9	28.4	16.4	40.4	28.2	10.3	35.7	19.8	11.7	36.8	18.5	
SE Eur	4.9	8.9	17.8	18.8	14.4	43.3	22.0	14.2	41.1	29.0	11.0	42.3	25.1	11.7	41.8	22.0	
Overall	−6.2	−12.7	−18.2	−18.3	−27.1	−30.4	−25.1	−17.4	−33.2	−24.7	−18.2	−32.1	−21.6	−26.2	−36.2	−26.8	
Land	−6.9	−10.7	−18.3	−18.8	−19.3	−38.3	−22.1	−18.5	−35.0	−26.2	−13.7	−34.3	−20.8	−15.7	−36.4	−21.9	
Sea	−5.6	−14.8	−18.0	−17.8	−35.0	−22.3	−28.2	−16.2	−31.5	−23.2	−22.9	−29.9	−22.4	−37.0	−36.0	−31.8	
GB-IR-IC	−6.6	−19.4	−18.0	−19.3	−23.2	−26.3	−28.8	−18.8	−32.0	−25.3	−19.9	−34.5	−23.6	−14.1	−33.7	−21.4	Geographical average of minimum negative fractional deviation for 1958–2001
Scandinavia	−7.6	−12.5	−21.2	−21.0	−18.4	−37.1	−28.7	−22.2	−29.0	−25.8	−14.4	−26.7	−20.1	−20.0	−30.6	−24.9	
NE Eur	−6.9	−11.1	−17.2	−17.5	−18.7	−44.9	−20.1	−18.7	−25.6	−21.2	−13.3	−23.3	−17.1	−19.5	−27.5	−20.4	
SW Eur	−6.4	−8.6	−15.9	−16.9	−13.8	−31.1	−21.2	−14.1	−39.5	−27.0	−10.7	−41.4	−19.9	−9.5	−43.6	−16.7	
SC Eur	−7.5	−8.7	−14.5	−15.3	−13.5	−35.5	−18.7	−13.5	−32.7	−22.6	−9.1	−31.3	−17.0	−10.3	−31.9	−15.8	
SE Eur	−5.2	−8.5	−13.8	−14.3	−12.5	−38.6	−16.3	−14.9	−36.4	−25.7	−11.1	−36.6	−21.3	−11.5	−37.7	−19.8	

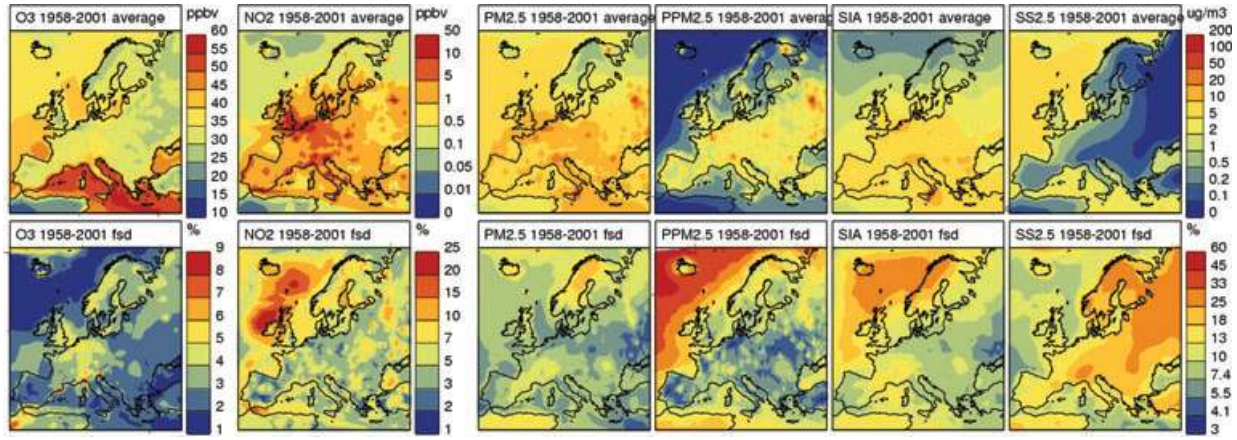

Fig. 2. Average of summer (April–September) ozone concentration and annual concentrations of nitrogen dioxide (NO_2), $PM_{2.5}$, primary $PM_{2.5}$ ($PPM_{2.5}$), secondary inorganic aerosol (SIA) and sea salt ($SS_{2.5}$) (units: O_3, NO_2: ppbv; $PM_{2.5}$, $PPM_{2.5}$, SIA, $SS_{2.5}$: μg m^{-3}) as well as fractional standard deviation (fsd) (unit: % of average) for the time period 1958–2001.

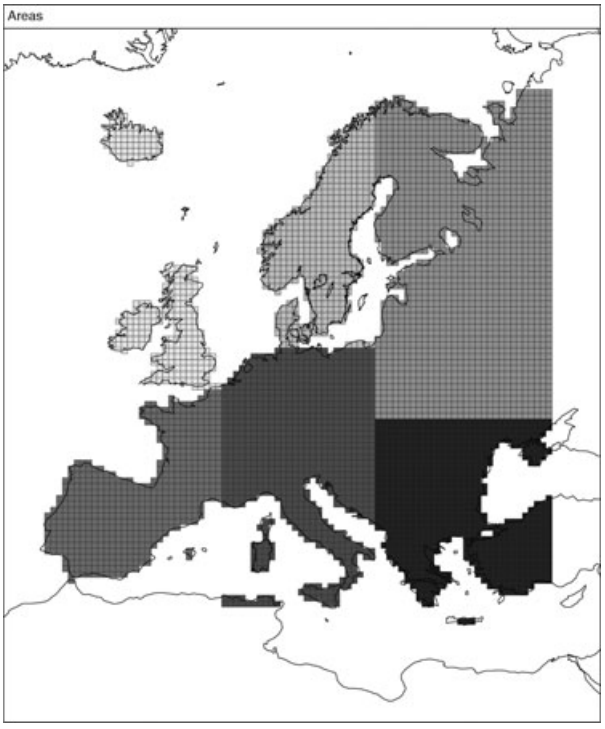

Fig. 3. Grey-scale indicating the six regions tabulated in Tables 5–8. From fair to dark: GB-IR-IC (northwest), Scandinavia (north-central), NE Eur (northeast), SW Eur (southwest), SC Eur (south-central), SE Eur (southeast).

for total precipitation and wind speed, whereas the picture is more complex for the other parameters. For temperature, the minimum deviation is greater in all regions except southeastern Europe. For cloud cover the minimum deviation is greater in northern Europe and for specific humidity, the minimum deviation is greater in the GB-IR-IC and northeastern Europe. This has the combined effect that for all deposition and concentrations except ozone, the average of the maximum deviation is greater than the average of the minimum deviation for all regions except southeastern Europe, for dry deposition of SO_x-S and NO_y-N. The average of the greatest deviation is a factor 2–3 greater than the fsd. The precipitation (wet deposition) and wind (dry deposition), therefore, seem to be important factors for deposition of nitrogen and sulphur as well as for PM and its constituents. SS is also complicated by emissions being dependent on temperature and wind; however, since the maximum deviation in SS over sea is greater, winds is the most important factor for the emissions. Formation of SIA and dry deposition of PM is also affected by humidity. Analysing the combined effect of the meteorological parameters is, however, outside the scope of this paper and will be left for future studies. Ozone is probably governed more by variation in temperature, hence the difference to the other airborne concentrations. This is probably in part due to variation in emissions and, therefore, concentration in isoprene (biogenic VOC). An analysis of the variation in isoprene will also be left for a future study.

The deviation in annual total deposition of NH_x-N, compared to the 44 yr average of annual total deposition is shown in Fig. 4. The deviation varies between −50% and 100% over larger areas, with a few exceptions. The pattern is similar for the total deposition of SO_x-S and NO_y-N (not shown). As seen in Fig. 5 the magnitude of wet deposition is generally larger than dry deposition. Hence the total deposition is dominated by the wet deposition and thus by precipitation. A comparison of the interannual variations in precipitation and wet deposition shows similar but not equal patterns (not shown). Especially in the regions where long-range transport dominates, for example, the North Sea and northern Scandinavia, wet deposition is less correlated with the precipitation amounts, due to the dependence on transport events from source regions. The interannual variations of wet and total deposition show very similar patterns, while the dry deposition differs much. The interannual variation in dry deposition varies between −50% and 100%, however, exceeding 100% over large

Table 6. Top section: average over regions for the period 1958–2001. Top middle section: Average over regions of fractional standard deviation (fsd). Bottom middle section: Average over regions of maximum fractional deviation. Bottom section: Average over regions of minimum fractional deviation. Units: average: Temp: °C, Total prec: mm d^{-1}, Wind speed: m s^{-1}, Cloud cover: 1, Spec Hum: g kg^{-1}; fsd and fractional deviation: % of 44 yr average (for temp.: % of K)

	T lev 1	Total prec	Wind speed	Cloud cover	Spec hum	
Overall	9.7	1.8	5.0	0.61	6.4	
Land	8.7	1.6	3.4	0.60	5.8	
Sea	10.8	2.0	6.6	0.62	6.9	
GB-IR-IC	7.4	2.1	5.1	0.74	5.6	
Scandinavia	3.6	2.0	3.5	0.71	4.5	Geographical average of average meteorological parameters
NE Eur	4.3	1.6	3.8	0.72	4.9	for 1958–2001
SW Eur	12.5	1.6	3.1	0.52	6.9	
SC Eur	9.7	1.8	3.1	0.60	6.4	
SE Eur	10.8	1.5	2.7	0.51	6.5	
Overall	0.22	23.6	4.7	6.5	2.0	
Land	0.26	24.9	4.9	7.2	2.6	
Sea	0.18	22.2	4.4	5.8	1.7	
GB-IR-IC	0.19	16.2	5.5	3.6	3.2	
Scandinavia	0.28	15.7	5.6	4.6	4.1	Geographical average of fractional standard deviation
NE Eur	0.35	15.8	4.5	4.1	4.3	for 1958–2001
SW Eur	0.20	28.0	4.6	9.2	3.4	
SC Eur	0.21	21.5	5.8	7.3	2.8	
SE Eur	0.21	23.5	4.3	8.4	3.3	
Overall	0.46	67.7	10.5	16.7	9.9	
Land	0.53	69.5	11.3	17.6	11.7	
Sea	0.38	65.9	9.6	15.8	8.0	
GB-IR-IC	0.41	33.8	11.9	7.5	7.8	Geographical average of maximum positive fractional deviation
Scandinavia	0.53	41.4	14.1	9.2	10.2	for 1958–2001
NE Eur	0.65	40.5	10.8	8.7	10.8	
SW Eur	0.43	74.0	10.8	20.7	11.1	
SC Eur	0.44	57.6	12.5	17.2	9.0	
SE Eur	0.48	59.9	9.9	20.5	12.2	
Overall	−0.50	−40.0	−9.8	−14.2	−9.3	
Land	−0.59	−42.3	−10.1	−15.9	−11.1	
Sea	−0.41	−37.6	−9.5	−12.4	−7.4	
GB-IR-IC	−0.42	−33.6	−11.8	−8.9	−10.1	Geographical average of minimum negative fractional deviation
Scandinavia	−0.64	−31.4	−10.8	−11.0	−9.9	for 1958–2001
NE Eur	−0.77	−31.1	−10.1	−10.7	−11.2	
SW Eur	−0.47	−44.7	−9.3	−19.0	−11.1	
SC Eur	−0.48	−41.4	−11.3	−16.8	−8.8	
SE Eur	−0.44	−46.3	−9.1	−18.4	−9.8	

areas over sea for NH_x-N. The average fsd for dry deposition is lower than for wet deposition in all regions except for NH_x-N over sea, as can be seen in Table 5.

The 44 yr average and fsd of annual wet and dry deposition for NH_x-N, NO_y-N and SO_x-S are shown in Fig. 5. The fsd of NH_x-N dry deposition is highest over sea, where the deposition is low. The 44 yr average of the annual total deposition is highest on the European continent, deposition of nitrogen being especially high in the Netherlands and northern Italy and the deposition of sulphur especially high in southern Italy and southeastern Europe. There is a strong gradient at the coast, especially for NH_x-N, which could explain the high values of fsd over sea.

4.2. Trends in concentrations and deposition

Figures 6 and 7 display linear trends in concentrations and deposition at 90% significance level. The trends in percent of the average concentration or average annual deposition per decade

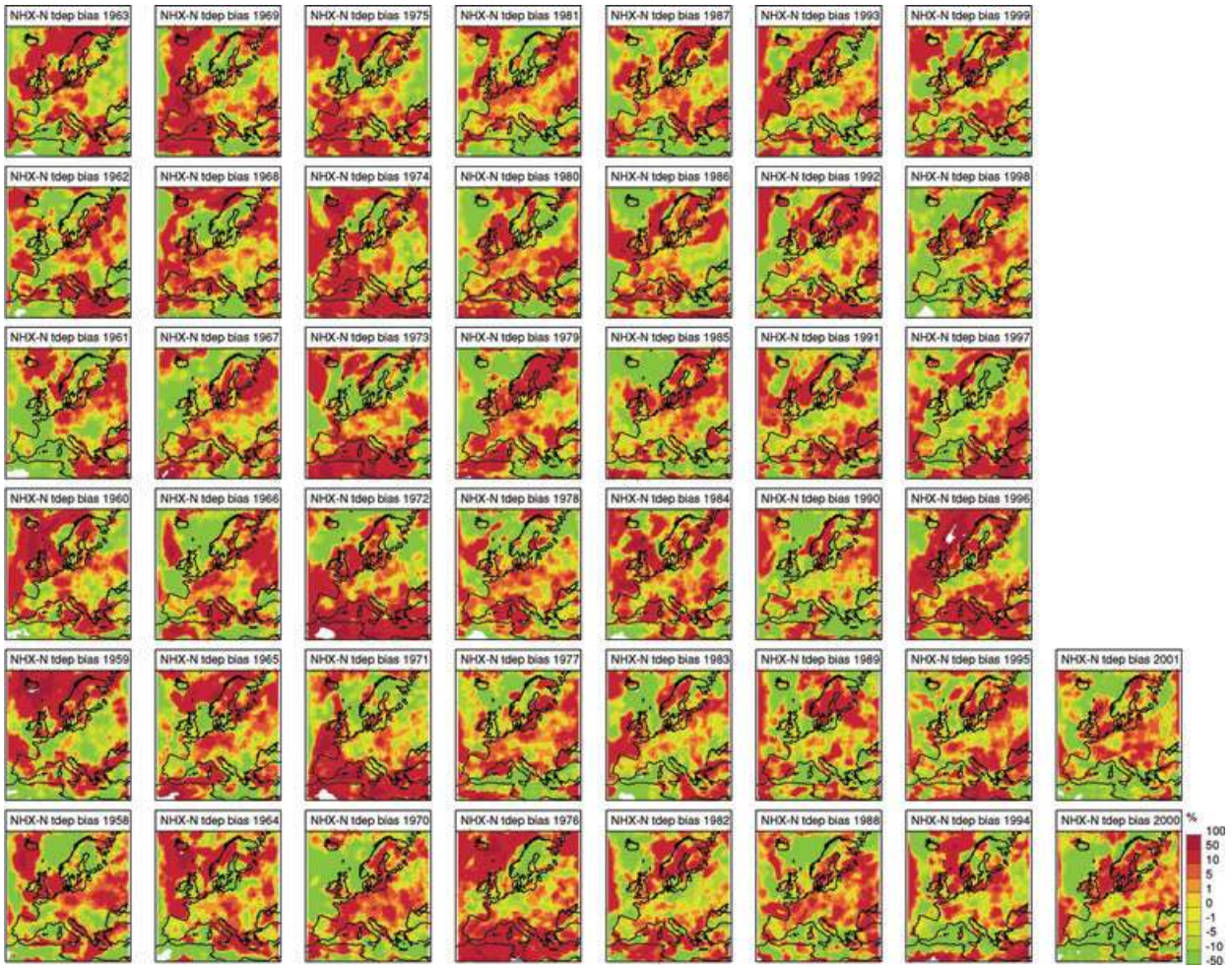

Fig. 4. Fractional bias (unit: %) of annual total deposition of reduced nitrogen compared to the 44 yr average (1958–2001).

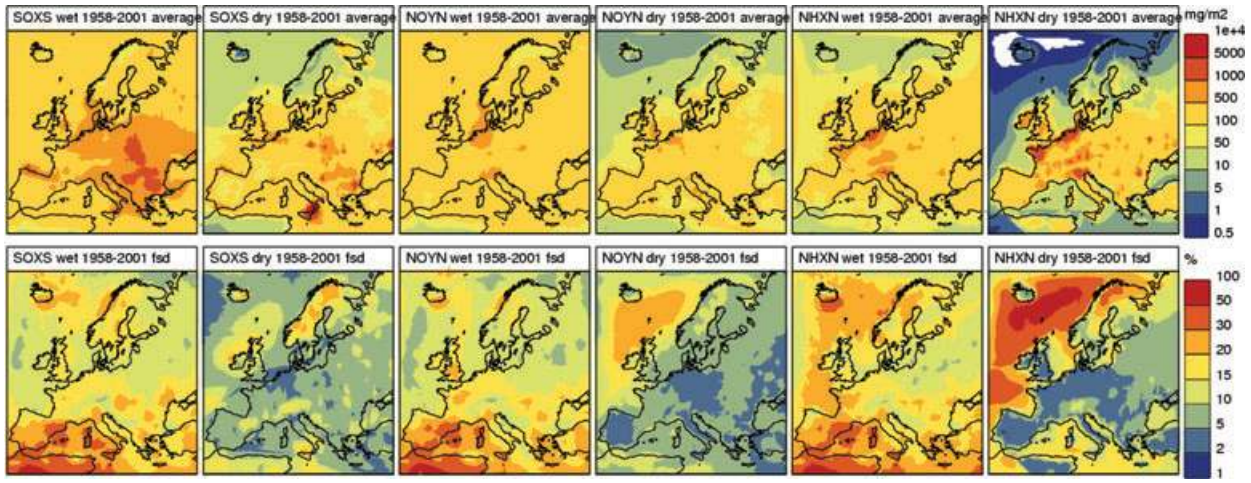

Fig. 5. Average of annual dry and wet deposition (unit: mg m^{-2}) as well as fractional standard deviation (fsd; unit: % of average) for reduced (NH_x-N) and oxidized (NO_y-N) nitrogen as well as oxidized sulphur (SO_x-S) for the time period 1958–2001.

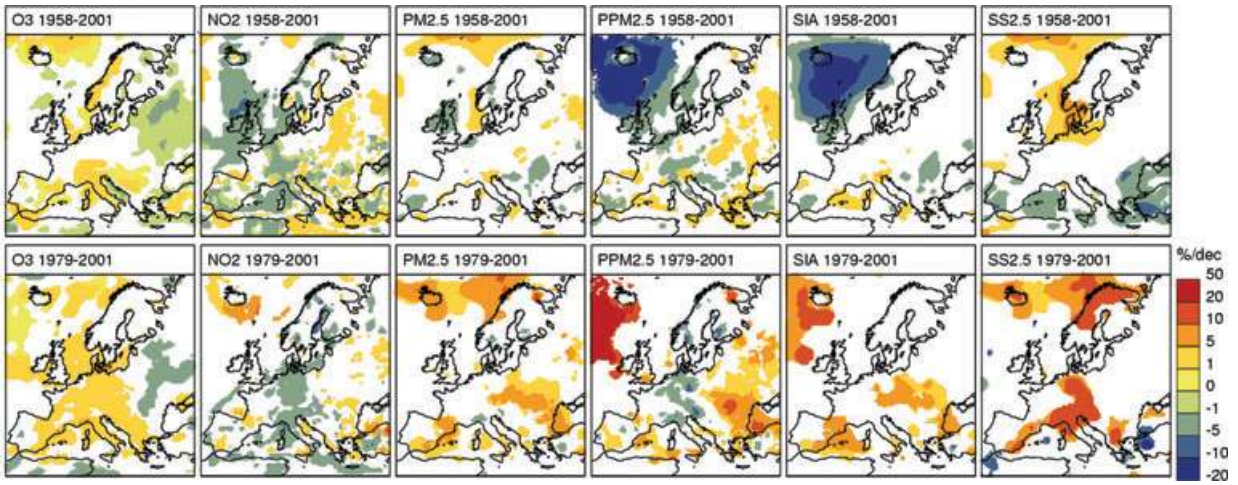

Fig. 6. Linear trends of air concentrations (unit: % per decade) at 90% significance level. White areas have no linear trend at 90% significance level. For the top row the time period is 1958–2001, for the bottom row time period is 1979–2001.

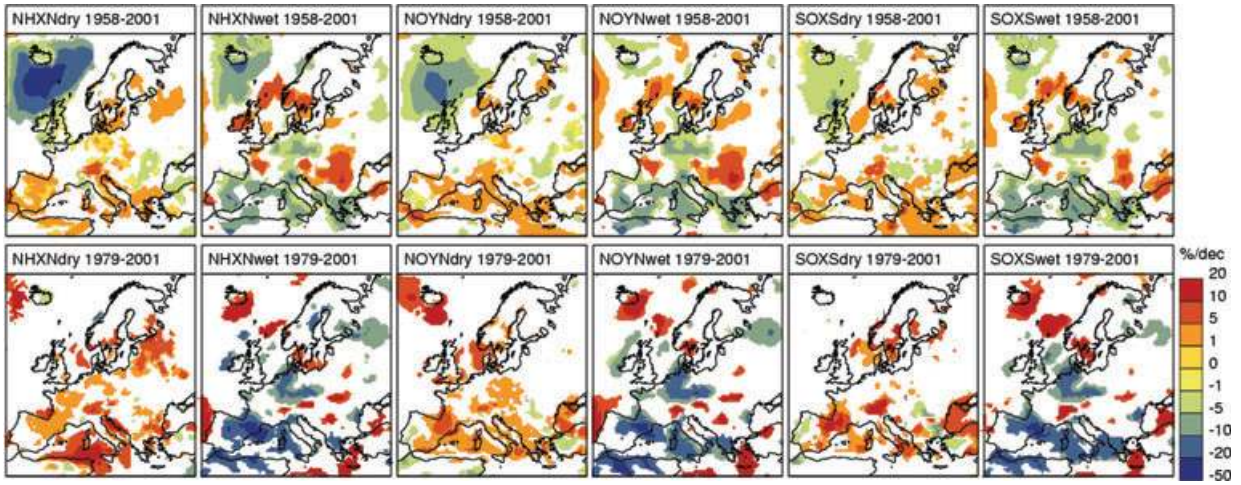

Fig. 7. Linear trends of deposition (unit: % per decade) at 90% significance level. White areas have no linear trend at 90% significance level. For the top row the time period is 1958–2001, for the bottom row the time period is 1979–2001.

are displayed for two periods: the top rows for the period 1958–2001 and the bottom rows for the period 1979–2001. The reason for choosing the second period is to reduce biases and trends in the data set due to the change in the amount of satellite data. However, it could still be biased due to improvements in the amount of data assimilated and due to the step change in 1988.

A significant trend can be seen in the ozone concentration over the years 1958–2001 for central and eastern Europe. However, the positive trend over the years 1979–2001 in ozone is more geographically widespread. In most parts of central and western Europe there is a change of +1% to +5% per decade during 1979–2001, while there is a negative trend between −1% and −5% per decade in some parts of eastern Europe. The positive trend in central Europe corresponds to an increase of +0.1 to +0.2 ppbv per year, whereas the negative trend corresponds to between −0.01 and −0.1 ppbv per year. This can be compared to the (possible) trend in background concentration: about 0.5 ppbv per year (Simmonds et al., 2004): only some of the background trend could be explained by a change in climate in the lower troposphere over Europe. The negative trend over Russia is more widely spread for the whole period 1958–2001, but stronger for the second period. The reason for the trends in ozone concentrations is a combination of change in temperature, wind patterns, cloud cover and stability. The present study does not allow us to draw conclusions about which processes that are most important. However, we will make some comparisons to trends in five meteorological parameters, which are displayed in Table 7.

To achieve more generalized information about the trends in average meteorological parameters, air pollution concentrations and deposition over regions, as indicated in Fig. 3, Tables 7 and 8 are considered. The reason for the trends being much weaker in Table 8 compared to the grid-point trends in Figs. 6 and 7 is that the table shows the trend in average concentration or deposition over a region, which tends to smooth spatial differences and

Table 7. Linear trends (unit: % per decade) in meteorological parameters. The top section refers to the time period 1958–2001, the middle section 1958–1978 and the bottom section 1979–2001. Trends at 90% significance level are given in bold. For temperature, the unit refers to percent Kelvin (K).

	T lev 1	Total prec	Wind speed	Cloud cover	Spec Hum	
Overall	0.01	**1.47**	**0.47**	−0.21	0.37	
Land	0.02	0.46	0.17	−0.31	0.44	
Sea	0.01	**2.30**	**0.62**	−0.10	0.31	
GB-IR-IC	0.01	**5.92**	**1.12**	**0.89**	**1.37**	
Scandinavia	0.02	**3.22**	**1.45**	0.24	0.48	Trend over 1958–2001
NE Eur	0.01	**2.28**	−0.33	0.31	0.31	
SW Eur	0.03	−2.13	−0.06	−0.65	**1.09**	
SC Eur	0.03	**−3.07**	**1.48**	−1.01	0.39	
SE Eur	−0.01	0.35	−0.15	−1.04	0.21	
Overall	**−0.13**	**13.04**	0.67	**5.19**	−0.07	
Land	**−0.14**	**13.49**	**1.35**	**5.86**	0.61	
Sea	**−0.12**	**12.66**	0.31	**4.52**	−0.65	
GB-IR-IC	**−0.08**	**6.92**	0.70	**2.89**	1.22	
Scandinavia	−0.05	**10.36**	1.19	**3.57**	0.96	Trend over 1958–1978
NE Eur	−0.16	**9.67**	**2.63**	**3.29**	**−2.64**	
SW Eur	**−0.15**	**20.59**	0.12	**9.15**	**2.77**	
SC Eur	−0.08	**9.72**	−0.08	**5.84**	−0.65	
SE Eur	**−0.16**	**14.43**	**1.61**	**7.93**	0.07	
Overall	**0.12**	**−1.99**	0.18	**−2.40**	**1.71**	
Land	**0.13**	**−3.73**	−0.19	**−3.04**	**1.37**	
Sea	**0.12**	−0.59	0.38	**−1.76**	**2.02**	
GB-IR-IC	**0.14**	−0.32	−0.61	−0.44	**2.46**	
Scandinavia	**0.17**	−0.11	**2.35**	−0.58	1.78	Trend over 1979–2001
NE Eur	0.13	−3.18	**−1.41**	**−1.87**	1.51	
SW Eur	**0.11**	**−6.63**	0.40	**−4.99**	0.07	
SC Eur	**0.13**	**−8.30**	**3.31**	**−4.12**	**2.07**	
SE Eur	**0.13**	2.39	**−1.76**	**−4.96**	**2.01**	

hence give less pronounced trends. Significant trends for ozone, at 90% significance level for the period 1958–2001, are found in central Europe (0.55% per decade) and in northeastern Europe (−0.55% per decade). For the second period 1979–2001 there are only significant positive trends for ozone: overall, over sea and in central and southwestern Europe. The only negative trend in ozone for this period is in northeastern Europe, but it is not significant at 90% significance level. Comparing to Table 7 we see that an increase in radiation due to less cloud cover and an increase in temperature in all regions could explain the positive trends during the second period. Both these affect the emissions of isoprene and hence the ozone formation, but they also affect the chemistry, for example, through photo dissociation of NO_2.

In Fig. 6 we see that there is a negative trend in NO_2 in central Europe during the whole period, and for smaller parts of eastern Europe the trend is positive, that is, to some extent the inverse of the trend in ozone. The negative trend in central Europe is more widespread for 1979–2001 and the absolute trend is higher than in the first period. The trend in NO_2 expressed in absolute values ranges between −0.05 and +0.05 ppbv. When studying Table 8 and Fig. 6 we see that the trend in NO_2 in general is opposite to the trend in O_3 mainly for the time period 1979–2001. This could be due to a change in the chemical balance between NO_2 and O_3, which could be induced by for example change in temperature and solar radiation. In Table 7 we see that the trend in temperature in central Europe is +0.13% per decade and in total cloud cover −4.12% per decade over the period 1979–2001, indicating that more solar radiation is available. The trend in temperature also affects the equilibrium between NO_2 and PAN, with lower temperatures more PAN is formed and could be transported elsewhere, and vice versa. The negative trend in both O_3 and NO_2 in most regions during the first period can probably be explained by lower temperatures, forming more PAN and emitting less isoprene, but it could also be due to increased dry deposition or other chemical reactions.

The trend in $PM_{2.5}$ is mostly positive for the period 1979–2001, but over land the significant trends are not widely spread. For the whole period only small regions display trends at all.

Table 8. Linear trends (unit: % per decade of average concentration or deposition) in air pollution concentrations and deposition. Index d stands for dry deposition, w for wet deposition and t for total (=wet + dry) deposition. The top section refers to the time period 1958–2001, the middle section 1958–1978 and the bottom section 1979–2001. Trends at 90% significance level are given in bold.

	O_3	NO_2	PM_{10}	$PM_{2.5}$	$PPM_{2.5}$	$SS_{2.5}$	SIA	SO_xSd	SO_xSw	SO_xSt	NO_yNd	NO_yNw	NO_yNt	NH_xNd	NH_xNw	NH_xNt	
Overall	0.08	**−0.52**	0.25	0.06	0.08	0.82	−0.38	0.32	**−1.05**	**−0.60**	0.03	−0.52	−0.34	0.14	−0.64	−0.31	
Land	0.01	**−0.43**	−0.06	−0.12	0.17	0.40	−0.31	0.22	**−0.98**	**−0.62**	0.03	−0.44	−0.26	0.18	−0.44	−0.15	
Sea	0.13	**−0.68**	0.47	0.22	−0.33	0.87	−0.48	**0.46**	**−1.16**	−0.59	0.01	−0.61	−0.46	−0.12	**−1.07**	**−0.84**	
GB-IR-IC	0.05	**−1.74**	**−1.52**	**−1.99**	**−2.07**	0.88	**−3.58**	**−1.48**	0.21	−0.37	**−1.73**	0.90	−0.19	**−1.04**	1.92	0.41	
Scandinavia	0.41	−0.49	0.38	−0.30	**−2.20**	**4.09**	−0.96	0.63	1.15	1.05	0.05	1.26	0.91	0.11	**2.13**	**1.49**	Trend over 1958–2001
NE Eur	**−0.57**	**0.60**	0.57	0.44	**1.47**	0.43	−0.49	0.41	−0.39	−0.20	−0.15	0.82	0.52	0.10	0.10	0.10	
SW Eur	0.34	**−0.62**	−0.11	−0.05	−0.24	−0.67	0.10	0.36	−1.90	−1.22	0.17	−1.45	−0.69	0.31	−0.81	−0.16	
SC Eur	**0.56**	**−0.66**	−0.00	0.05	**−0.85**	0.62	0.39	0.18	**−3.82**	**−2.27**	0.40	**−3.09**	**−1.63**	**0.44**	**−2.85**	**−1.19**	
SE Eur	0.15	0.06	−0.56	−0.55	0.10	**−3.23**	−0.69	0.24	0.94	0.72	−0.02	**2.44**	**1.50**	−0.09	**2.48**	**1.27**	
Overall	−0.5	**−1.0**	**−6.3**	**−7.1**	**−4.1**	**−4.6**	**−9.5**	**−2.1**	**3.7**	**1.9**	**−4.1**	**4.8**	**2.0**	**−2.2**	**4.7**	**1.9**	
Land	**−0.6**	**−0.7**	**−7.1**	**−7.4**	**−3.6**	**−12.2**	**−8.8**	**−1.9**	**3.7**	**2.0**	**−3.6**	**4.8**	**1.6**	**−1.9**	**5.6**	**2.1**	
Sea	−0.5	**−1.5**	**−5.7**	**−6.7**	**−6.1**	**−3.8**	**−10.4**	**−2.4**	**3.7**	1.6	**−5.2**	**4.8**	**2.5**	**−4.5**	2.7	1.0	
GB-IR-IC	0.0	**−3.5**	**−6.1**	**−6.1**	−4.2	**−7.3**	−6.0	−2.6	0.5	−0.6	−3.5	0.8	−1.1	**−2.0**	2.2	0.0	
Scandinavia	0.6	**−2.3**	**−9.1**	**−9.9**	**−7.0**	−4.4	**−13.4**	**−5.6**	**−6.4**	**−6.3**	**−6.3**	−2.4	**−3.5**	**−2.3**	−4.1	**−3.5**	Trend over 1958–1978
NE Eur	−0.2	−0.6	**−5.3**	**−5.6**	**−3.0**	**−18.1**	**−7.2**	**−2.3**	−1.7	−1.8	**−3.4**	0.0	−1.1	**−2.2**	0.4	−0.5	
SW Eur	−0.7	**−1.4**	**−8.6**	**−8.6**	**−3.9**	**−15.4**	**−9.5**	**−3.2**	**16.0**	**10.4**	**−4.3**	**19.3**	**8.6**	**−2.7**	**22.7**	**8.1**	
SC Eur	**−1.8**	0.5	**−5.4**	**−5.5**	**−2.3**	**−13.6**	**−6.4**	−1.2	1.1	0.2	**−2.3**	2.2	0.3	−1.0	1.9	0.4	
SE Eur	−0.9	**−0.7**	**−8.4**	**−8.7**	**−5.5**	**−14.3**	**−9.6**	−0.7	**8.4**	**5.5**	**−4.1**	**8.1**	**3.5**	**−2.3**	**9.5**	**3.9**	
Overall	**0.58**	**−0.78**	1.41	**1.59**	**1.67**	1.27	1.75	**1.36**	**−2.00**	−0.89	**1.44**	**−1.81**	**−0.75**	**1.38**	**−2.53**	**−0.89**	
Land	0.44	**−0.70**	**1.89**	**1.77**	**1.62**	3.14	1.70	**1.24**	**−2.65**	**−1.45**	**1.21**	**−3.01**	**−1.39**	**1.37**	**−3.21**	**−1.03**	
Sea	**0.68**	−0.93	1.06	1.43	**1.89**	1.07	1.81	**1.51**	−0.97	−0.08	**1.98**	−0.44	0.15	**1.48**	−1.01	−0.41	
GB-IR-IC	0.81	0.79	1.85	2.23	2.76	2.15	2.08	0.90	−1.93	−0.99	2.41	−0.74	0.54	0.69	−2.56	−0.94	
Scandinavia	0.46	−1.15	1.74	1.06	−1.86	6.13	0.53	**3.11**	3.66	3.55	2.25	1.81	1.94	0.66	1.31	1.11	Trend over 1979–2001
NE Eur	−0.60	0.30	**2.75**	**2.14**	**3.63**	6.02	0.57	1.71	−0.96	−0.33	0.46	−1.16	−0.66	**2.27**	−1.38	−0.05	
SW Eur	**1.15**	−0.09	1.83	1.99	0.58	1.77	2.52	**1.84**	**−7.48**	**−4.57**	**2.03**	**−7.56**	**−2.95**	**1.51**	**−8.61**	**−2.61**	
SC Eur	**2.16**	**−2.08**	1.03	1.13	**−1.77**	**5.59**	2.05	**1.76**	**−5.56**	**−2.64**	**1.34**	**−6.12**	**−2.93**	**1.22**	**−5.24**	**−1.91**	
SE Eur	0.44	**0.60**	**2.35**	**2.43**	**3.60**	0.15	2.09	−0.03	−1.07	−0.74	0.62	0.85	0.76	0.92	0.62	0.76	

Over land the trend in $PM_{2.5}$ mostly shows the same pattern as SIA and over sea the trend is similar to the trend in SS. For SS the trend is negative over parts of the Mediterranean area for the whole 44 yr period. For the period 1979–2001 the significant trends in SS are positive, except for a small region over and close to Turkey. The trend in $PPM_{2.5}$ is similar to the trend in NO_2; positive in eastern Europe and negative in central Europe. There are differences between PPM and NO_2: for example, the dry deposition velocities and the fact that NO_2 is chemically reactive forming PAN and photo dissociating to NO. The fact that the patterns in the trends are similar despite this need further studies to be explained.

The significant trends in $PPM_{2.5}$ in the second period are opposite to those in wind, except for the averages over the whole domain: land and sea, showing that change in dry deposition is the main reason for the change in $PPM_{2.5}$ over land, as expected. $PPM_{2.5}$ shows a geographically more widespread trend than $PM_{2.5}$ and the other constituents, which is also seen in Table 8, but the trend in SIA compensates the trend in $PPM_{2.5}$ in south-central Europe and since SIA displays higher concentrations in larger areas, the trend in $PM_{2.5}$ is mainly governed by SIA. The reason for the opposite trends in SIA and PPM could be that the higher humidity together with more ozone increases the oxidizing capacity, creating more SIA, while the humidity acts as a sink for PPM since the humidity increases its dry deposition velocity.

In Table 8 we also see that for almost all regions the air concentrations of aerosol and chemical species are increasing during the 1979–2001 period. The exceptions are $PPM_{2.5}$ for south-central Europe and NO_2 (in all significant regions except southeastern Europe). During the first subperiod 1958–1978 the significant trends are negative for air concentrations of all chemical compounds and aerosol, as well as for dry deposition of sulphur and nitrogen, while wet deposition of sulphur and nitrogen mostly increased except for sulphur in Scandinavia. However, this period could be biased by a change in amount of satellite data used, as described earlier.

When comparing to the observed trends in sulphate in particles in air, described in section 1, we see that part of the missing decrease could be due to meteorological variation. The increase in SIA in southern Europe, which is probably due to a decrease in precipitation in ERA40, could in part act against the decrease of sulphur and nitrogen emissions.

There are trends towards higher dry deposition in NH_x-N, SO_x-S and NO_y-N over land for the period 1979–2001, which can be seen in both Fig. 7 and in Table 8, whereas the first period displays decreasing trends in most regions. The wet deposition displays decreasing patterns in most parts of southern and western Europe for the second period, but as seen in Table 8 the negative trend in wet deposition is only significant in southwestern and central Europe. Comparing to the trend in the ERA40 precipitation for the time period 1979–2001 we have negative trends in precipitation in ERA40 over southwestern and central Europe. These trends are not as pronounced in the GPCP data; however; the trend in southwestern Europe is positive even in the GPCP data. Hence this pattern could, to some extent, be an artificial effect. Decreasing precipitation in southern and western parts of Europe, as present in the ERA40 data set, would mean a decrease in wet deposition as well as an increase in concentrations in air and subsequent increase in dry deposition. Moreover, the increased concentration in air in western and southern Europe would also mean higher concentrations in air in northern Europe due to an increase in transported sulphur and nitrogen to the north. The trend in total deposition is very similar to the trend in wet deposition. The reason for this is that the wet deposition is higher overall than the dry deposition.

5. Conclusions

Interannual variability of O_3, NO_2, $PM_{2.5}$, PM_{10}, SIA, $SS_{2.5}$, $PPM_{2.5}$ and deposition of NH_x-N, NO_y-N and SO_x-S over Europe, due to climate variability, has been studied for the period 1958–2001, using a CTM driven by the ERA40 re-analysis. The study revealed that the average European land-area interannual variation, due to meteorological variability, ranges from 3% for O_3, 5% for NO_2, 9% for PM and primary PM, 6–9% for dry deposition of sulphate and nitrogen, 11% for secondary inorganic aerosol, 11–14% for total deposition to about 20% for wet deposition of sulphur and nitrogen and SS concentrations. During the years 1958–1978 the dry deposition and air concentrations display decreasing trends omitting changes in emission, whereas the trend in average wet and total deposition is increasing in most parts of Europe. However, the trends for this period might be biased by a change in number of observations used in the data assimilation. For the period 1979–2001 there are positive trends in ozone in central and southwestern Europe and negative trends in northeastern Europe. The trend in NO_2 is approximately opposite to that of O_3 and the trend in PM is positive in eastern Europe. There are negative trends in wet deposition in southwestern and central Europe and positive trends in dry deposition overall but these could be artificial. A bias in ERA40 precipitation could be partly responsible for the trends in wet deposition, and perhaps also to some extent the dry deposition and concentrations of gaseous chemical compounds and PM since the precipitation affects all these parameters.

Further investigation is needed to separate the relative importance of different meteorological parameters to the trends, as well as the importance of climate change versus hemispheric transport and emission reductions. It is important to investigate the relative importance of different meteorological parameters in order to make it possible to explain whether the observed trends in the data set are applicable in reality because of the difference in trends in precipitation between GPCP and ERA40. Such a study would reveal for example what impact the precipitation underestimation has on the air pollution budgets. Such a study would also be of general interest to learn more about which

processes are most important for the concentration and deposition of air pollutants; for example, to which extent the total deposition is influenced by precipitation.

The trend in ozone indicates that trends observed in ozone at sites throughout Europe are affected not only by changes in ozone-precursor emissions and hemispheric transport, but also a change in climate even at decadal timescales. This is true for all concentrations and deposition investigated. The importance of the precipitation versus other meteorological components used from the ERA40 data set such as temperature, for which trends probably are more accurate, will have to be investigated further. The importance of emission reduction and hemispheric transport on trends in air pollution versus the importance of climate change also need further studies. All compounds investigated display significant trends over the time periods. This indicates that climate variability has an importance for the chemical balance in the troposphere. This also implies that we can expect changes in the future, due to climate change. There is a need for improved re-analysis data sets for future studies.

In essence the following conclusions can be drawn from this paper:

(1) There is a high interannual variation in the surface concentrations and deposition of pollutants, that is, design of measurement campaigns and interpretation of measured data should be conducted carefully.

(2) Decadal variation exists: what is measured now will probably not be valid (given the same emissions) in 10 yr.

(3) Trends over longer time periods (>20 yr) exist. The trends differ between the constituents. These trends could mask emission reductions. It is important to eliminate trends due to climate variability in measured time-series before interpretation of trends due to emission changes can be done.

(4) In deciding on emission reductions for the future, possible climate-change induced changes of air pollution need to be considered.

6. Acknowledgements

This study was financed partly by the project Network for the support of European Policies on Air Pollution (NEPAP), which was supported by the European Commission through the contract EVK2-CT-2002–80019. Special thanks to Valentin Foltescu, SMHI, for the processed measurement data and to colleagues at SMHI for their support.

7. Appendix

In Table 9 boundary values for all non-zero species, except H_2O_2, N_2O_5 and HNO_3 are displayed. For these the method is somewhat different; based partly on results from model simulations profiles of HNO_3 (Kraus et al., 1996), N_2O_5 (Dameris et al., 1998; Kanakidou et al., 1991) and H_2O_2 (De Serves et al., 1994; Chin et al., 1996) at different latitudes were used. For PAN, results from a large-scale simulation (Moxim et al., 1996) are used. The lateral O_3 boundary concentrations are based on

Table 9. Boundary conditions for all species with non-zero boundary values, except for H_2O_2, N_2O_5 and HNO_3. NMVOCs are lumped and should not be regarded as the species indicated. Unit: mole mol^{-1}.

Model Component	Month	c_{top}	c_{west}	c_{east}	c_{south}	c_{north}
NO		1.00E−11	1.00E−11	1.00E−11	1.00E−11	1.00E−11
NO_2		3.00E−11	3.00E−10	1.00E−09	3.00E−10	1.00E−10
NH_3		5.00E−11	1.00E−10	5.00E−10	1.00E−10	1.00E−10
H_2		5.00E−07	5.00E−07	5.00E−07	5.00E−07	5.00E−07
C_3H_6		5.00E−11	5.00E−11	2.00E−10	1.60E−11	2.00E−10
HCHO		4.30E−11	4.90E−10	7.50E−10	2.40E−10	2.40E−10
CH_3CHO		1.40E−10	2.00E−10	3.20E−10	1.40E−10	1.40E−10
$CH_3COC_2H_5$		2.50E−11	2.50E−11	5.00E−11	2.50E−11	2.50E−11
CH_3O_2H		7.50E−11	1.00E−10	1.00E−10	1.00E−10	1.00E−12
MGLYOX		0.00E+00	2.00E−12	1.50E−11	2.00E−12	2.00E−12
GLYOX		0.00E+00	6.00E−12	1.30E−11	4.00E−12	4.00E−12
C_5H_8		0.00E+00	1.00E−11	1.50E−10	3.00E−10	3.00E−11
C_2H_5OH		4.00E−10	4.00E−10	6.00E−10	7.00E−11	4.00E−10
C_2H_5OOH		1.00E−12	1.00E−12	1.00E−12	1.00E−12	1.00E−12
CH_3OH		5.00E−11	5.00E−11	7.00E−11	8.00E−12	5.00E−11
SO_2	Jan	4.00E−11	3.20E−10	3.00E−10	4.00E−11	5.50E−10
	Feb	4.00E−11	2.00E−10	3.00E−10	4.00E−11	1.20E−10
	Mar	4.00E−11	2.10E−10	3.00E−10	4.00E−11	8.80E−10
	Apr	4.00E−11	1.20E−10	3.00E−10	1.20E−10	1.20E−10
	May–Sep	4.00E−11	4.00E−11	3.00E−10	4.00E−11	4.00E−11
	Oct	4.00E−11	5.60E−11	3.00E−10	4.00E−11	4.20E−11

Table 9. Continued.

Model Component	Month	c_{top}	c_{west}	c_{east}	c_{south}	c_{north}
	Nov	4.00E−11	3.60E−11	3.00E−10	4.00E−11	6.50E−11
	Dec	4.00E−11	4.90E−11	3.00E−10	4.00E−11	2.40E−10
CO	Jan	1.20E−07	1.50E−07	1.70E−07	1.20E−07	1.60E−07
	Feb	1.30E−07	1.60E−07	1.90E−07	1.30E−07	1.70E−07
	Mar	1.30E−07	1.60E−07	2.00E−07	1.30E−07	1.80E−07
	Apr	1.30E−07	1.60E−07	1.90E−07	1.30E−07	1.70E−07
	May	1.10E−07	1.40E−07	1.60E−07	1.10E−07	1.40E−07
	June	9.10E−08	1.10E−07	1.10E−07	9.10E−08	1.10E−07
	July	8.00E−08	9.50E−08	8.50E−08	8.00E−08	8.70E−08
	Aug	2.00E−08	1.00E−07	9.20E−08	8.20E−08	8.90E−08
	Sep	8.50E−08	1.10E−07	1.10E−07	8.50E−08	1.00E−07
	Oct	8.70E−08	1.10E−07	1.30E−07	8.50E−08	1.10E−07
	Nov	9.60E−08	1.30E−07	1.40E−07	9.60E−08	1.20E−07
	Dec	1.10E−07	1.40E−07	1.60E−07	1.10E−07	1.40E−07
CH_4	Jan	1.76E−06	1.82E−06	1.82E−06	1.76E−07	1.84E−06
	Feb	1.77E−06	1.80E−06	1.80E−06	1.77E−07	1.84E−06
	Mar	1.78E−06	1.81E−06	1.81E−06	1.78E−07	1.83E−06
	Apr	1.77E−06	1.81E−06	1.81E−06	1.77E−07	1.82E−06
	May	1.76E−06	1.81E−06	1.81E−06	1.76E−07	1.81E−06
	June	1.77E−06	1.79E−06	1.79E−06	1.77E−07	1.79E−06
	July	1.76E−06	1.78E−06	1.78E−06	1.76E−07	1.79E−06
	Aug	1.74E−06	1.79E−06	1.79E−06	1.74E−07	1.79E−06
	Sep	1.75E−06	1.79E−06	1.79E−06	1.75E−07	1.80E−06
	Oct	1.77E−06	1.81E−06	1.81E−06	1.77E−07	1.81E−06
	Nov	1.78E−06	1.82E−06	1.82E−06	1.78E−07	1.82E−06
	Dec	1.77E−06	1.82E−06	1.82E−06	1.77E−07	1.82E−06
C_2H_6	Jan	2.60E−09	2.60E−09	3.00E−09	1.20E−09	3.50E−09
	Feb	3.00E−09	3.00E−09	3.00E−09	1.40E−09	3.50E−09
	Mar	3.30E−09	3.30E−09	3.30E−09	1.50E−09	3.50E−09
	Apr	3.30E−09	3.60E−09	3.30E−09	1.70E−09	3.30E−09
	May	2.40E−09	3.10E−09	2.00E−09	1.70E−09	2.40E−09
	June	1.70E−09	2.20E−09	2.00E−09	1.40E−09	1.70E−09
	July	1.40E−09	1.30E−09	2.00E−09	1.00E−09	1.40E−09
	Aug	1.40E−09	1.60E−09	2.00E−09	1.00E−09	1.40E−09
	Sep	1.70E−09	1.90E−09	2.00E−09	1.00E−09	1.70E−09
	Oct	1.80E−09	2.00E−09	2.00E−09	1.00E−09	1.80E−09
	Nov	2.00E−09	2.00E−09	2.00E−09	1.00E−09	1.90E−09
	Dec	2.20E−09	2.30E−09	2.20E−09	1.10E−09	2.70E−09
NC_4H_{10}	Jan	6.00E−10	6.00E−10	2.00E−09	1.60E−10	3.00E−09
	Feb	1.00E−09	8.00E−10	2.00E−09	1.90E−10	2.90E−09
	Mar	1.20E−09	9.50E−10	2.00E−09	2.20E−10	3.10E−09
	Apr	1.10E−09	1.10E−09	1.10E−09	2.50E−10	1.40E−09
	May	3.20E−10	4.60E−10	1.00E−09	1.60E−10	3.20E−10
	June	1.60E−10	2.90E−10	1.00E−09	1.30E−10	1.30E−10
	July	1.00E−10	1.20E−10	1.00E−09	1.00E−10	1.00E−10
	Aug	1.40E−10	1.90E−10	1.00E−09	1.00E−10	1.40E−10
	Sep	3.20E−10	3.50E−10	1.00E−09	5.00E−11	3.40E−10
	Oct	3.00E−10	3.00E−10	1.00E−09	1.00E−10	7.10E−10
	Nov	3.00E−10	3.00E−10	1.00E−09	1.00E−10	1.00E−09
	Dec	5.00E−10	4.00E−10	1.50E−09	1.30E−10	2.00E−09
C_2H_4	Jan	2.60E−10	2.60E−10	3.40E−10	5.00E−11	5.30E−10
	Feb	3.30E−10	2.90E−10	3.60E−10	5.00E−11	4.40E−10
	Mar	3.10E−10	3.40E−10	4.00E−10	5.00E−11	3.10E−10

Table 9. Continued.

Model Component	Month	c_{top}	c_{west}	c_{east}	c_{south}	c_{north}
	Apr	3.40E−10	3.40E−10	2.80E−10	5.00E−11	2.30E−10
	May	1.90E−10	1.90E−10	2.00E−10	5.00E−11	1.80E−10
	June	1.70E−10	1.80E−10	2.00E−10	5.00E−11	1.70E−10
	July	1.40E−10	1.80E−10	2.00E−10	5.00E−11	1.40E−10
	Aug	2.00E−10	1.70E−10	2.00E−10	5.00E−11	2.00E−10
	Sep	2.00E−10	2.00E−10	2.00E−10	5.00E−11	2.00E−10
	Oct	2.00E−10	2.00E−10	2.00E−10	5.00E−11	2.70E−10
	Nov	2.00E−10	2.00E−10	2.00E−10	5.00E−11	3.00E−10
	Dec	2.30E−10	2.30E−10	3.20E−10	5.00E−11	4.50E−10
o-XYLENE	Jan	2.20E−10	2.20E−10	4.00E−10	4.00E−11	6.00E−10
	Feb	3.20E−10	2.80E−10	4.00E−10	4.00E−11	5.00E−10
	Mar	3.40E−10	3.40E−10	4.00E−10	4.00E−11	5.00E−10
	Apr	4.00E−10	4.00E−10	4.00E−10	4.00E−11	5.00E−10
	May	2.30E−10	1.20E−10	2.00E−10	4.00E−11	2.30E−10
	June	1.40E−10	7.50E−11	2.00E−10	4.00E−11	1.40E−10
	July	1.40E−10	3.10E−11	2.00E−10	4.00E−11	1.40E−10
	Aug	1.50E−10	6.60E−11	2.00E−10	4.00E−11	1.80E−10
	Sep	1.80E−10	7.90E−11	2.00E−10	4.00E−11	1.80E−10
	Oct	2.00E−10	1.00E−10	2.00E−10	4.00E−11	2.00E−10
	Nov	2.00E−10	1.00E−10	2.00E−10	4.00E−11	2.60E−10
	Dec	1.60E−10	1.60E−10	3.00E−10	4.00E−11	4.30E−10
O_3 (1999)	Jan	5.10E−08	3.70E−08	3.40E−08	3.80E−08	3.50E−08
	Feb	5.50E−08	4.00E−08	3.30E−08	3.60E−08	4.10E−08
	Mar	5.90E−08	4.50E−08	4.80E−08	4.70E−08	4.50E−08
	Apr	6.60E−08	4.50E−08	4.60E−08	4.60E−08	4.50E−08
	May	7.40E−08	4.10E−08	4.40E−08	4.80E−08	4.10E−08
	June	7.30E−08	3.70E−08	4.30E−08	4.40E−08	3.60E−08
	July	6.70E−08	3.10E−08	3.40E−08	3.40E−08	2.90E−08
	Aug	6.20E−08	3.10E−08	3.70E−08	3.40E−08	2.90E−08
	Sep	5.90E−08	3.00E−08	4.20E−08	3.40E−08	2.70E−08
	Oct	5.50E−08	3.20E−08	3.10E−08	3.40E−08	2.90E−08
	Nov	5.50E−08	3.50E−08	2.70E−08	3.60E−08	3.20E−08
	Dec	5.10E−08	3.50E−08	2.40E−08	3.70E−08	3.60E−08
SO_4^{2-}	Jan	1.00E−12	2.70E−10	1.00E−12	2.50E−10	2.30E−10
	Feb	1.00E−12	7.70E−10	1.00E−12	2.50E−10	3.20E−10
	Mar	1.00E−12	2.70E−10	1.00E−12	2.50E−10	4.50E−10
	Apr	1.00E−12	1.20E−10	1.00E−12	2.50E−10	1.60E−10
	May	2.60E−11	1.50E−10	4.00E−10	3.00E−10	9.00E−11
	June	2.60E−11	1.50E−10	4.00E−10	3.00E−10	7.00E−11
	July—Aug	2.60E−11	1.50E−10	4.00E−10	3.00E−10	3.00E−11
	Sep	1.00E−12	1.25E−10	1.20E−12	2.50E−10	5.00E−11
	Oct	1.00E−12	2.75E−10	1.00E−12	2.50E−10	1.00E−10
	Nov	1.00E−12	2.75E−10	1.00E−12	2.50E−10	1.90E−10
	Dec	1.00E−12	2.75E−10	1.00E−12	2.50E−10	2.40E−10
PAN	Jan	2.20E−10	2.50E−10	4.00E−10	4.40E−11	2.90E−10
	Feb	2.50E−10	2.60E−10	4.00E−10	5.90E−11	3.60E−10
	Mar	2.80E−10	2.80E−10	3.00E−10	6.90E−11	2.80E−10
	Apr	3.00E−10	3.00E−10	3.00E−10	6.00E−11	3.00E−10
	May	3.00E−10	2.00E−10	3.00E−10	6.00E−11	2.00E−10
	June	2.00E−10	1.00E−10	2.00E−10	5.00E−11	1.00E−10
	July	1.50E−10	5.00E−11	2.00E−10	3.00E−11	3.00E−11
	Aug	1.50E−10	8.00E−11	2.00E−10	3.00E−11	7.00E−11

Table 9. Continued.

Model Component	Month	c_{top}	c_{west}	c_{east}	c_{south}	c_{north}
	Sep	1.50E−10	1.00E−10	3.00E−10	3.00E−11	1.00E−10
	Oct	1.50E−10	1.50E−10	3.00E−10	5.00E−11	1.50E−10
	Nov	1.80E−10	1.80E−10	3.00E−10	5.30E−11	2.00E−10
	Dec	2.00E−10	2.20E−10	4.00E−10	4.60E−11	2.40E−10
NO_3^-	Jan–Sep	2.50E−11	1.70E−10	1.00E−12	1.50E−10	2.50E−11
	Oct–Dec	2.50E−11	1.75E−10	1.00E−12	1.50E−10	2.50E−11
NH_4NO_3	Jan	2.50E−11	2.50E−11	4.00E−10	5.00E−11	5.00E−11
	Feb–Dec	2.50E−11	2.50E−11	2.00E−10	5.00E−11	2.50E−11
$(NH_4)_2SO_4$	Jan–Aug	2.50E−11	2.50E−11	4.00E−10	5.00E−11	2.00E−11
	Sep–Dec	2.50E−11	2.50E−11	4.00E−10	3.00E−10	3.00E−11

back-trajectory analysed measurement data for 1999 from EMEP measurement stations and the top concentrations on sonde data from Norway, UK and Ireland (average for the years 1996–2001).

References

Andersson, C. and Largner, J. 2005. Interannual variations of ozone and nitrogen dioxide over Europe during 1958–2003 simulated with a regional CTM. Accepted to the Acid Rain, 2005, Journal special issue of Focus: Water, Air and Soil Pollution.

Andersson, E., Beljaars, A., Chevallier, F., Hólm, E., Janisková, M. and co-authors. 2005. Assimilation and modelling of the hydrological cycle in the ECMWF forecasting system. *Bull. Am. Meteorol. Soc.* **86**, 387–402.

Bengtsson, L., Hagemann, S. and Hodges, K. I. 2004. Can climate trends be calculated from reanalysis data? *J. Geophys. Res.* **109**(D11), D11111, doi:10.1029/2004JD004536

Berge, E. 1993. Coupling of wet scavenging of sulphur to clouds in a numerical weather prediction model. *Tellus* **45B**, 1–22.

Bott, A. 1989. A positive definite advection scheme obtained by nonlinear renormalization of advective fluxes. *Month. Weath. Rev.* **117**, 1006–1015.

Carter, W. P. L. 1996. Condensed atmospheric photo oxidation mechanisms for isoprene. *Atmosph. Env.* **30**, 4275–4290.

Chin, M., Jacob, D. J., Gardner, G. M., Foreman-Fowler, M. S. and Spiro, P. A. 1996. A global three-dimensional model of tropospheric sulphate. *J. Geophys. Res.* **101**(D13), 18 667–18 690.

Dameris, M., Grewe, V., Köhler, R., Sausen, R., Brühl, C. and co-authors. 1998. Impact of aircraft NO_x emissions on tropospheric and stratospheric ozone. Part II: 3-D model results. *Atmosph. Env.*, 3185–3199.

Dana, M. T. and Hales, J. M. 1976. Statistical aspects of the washout of polydisperse aerosols. *Atm. Env.* **10**, 45–50.

De Serves, C. 1994. Gas phase formaldehyde and peroxide measurements in the Arctic atmosphere. *J. Geophys. Res.* **99**(D12), 25 391–25 398.

EMEP/CCC, 1999. EMEP measurement data. URL: http://www.emep.int, Jan. and Jul. 2001 (ozone) and Apr. 2003 (other compounds).

Foltescu, V. L., Pryor, C. S. and Bennet, C. 2005. Sea salt generation, dispersion and removal on the regional scale. *Atm. Env.* **39**, 2123–2133.

Fusco, A. C. and Logan, J. A. 2003. Analysis of 1970–1995 trends in tropospheric ozone at Northern Hemisphere midlatitudes with the GEOS-CHEM model. *J. Geophys. Res.* **108**(D15), 4449–4473.

Gidhagen, L., Johansson, C., Langner, J. and Foltescu, V. L. 2005. Urban scale modeling of particle number concentration in Stockholm. *Atm. Env.* **39**, 1711–1725.

Gong, S. L., Barrie, L. A. and Blanchet, J.-P. 1997. Modeling sea-salt aerosols in the atmosphere. 1. Model development. *J. Geophys. Res.* **102**(D3), 3805–3818.

Grennfelt, P. and Hov, O. 2005. Regional air pollution at a turning point. *Ambio* **34**(1), 2–10.

Hagemann, S., Arpe, K. and Bengtsson, L. 2005. Validation of the hydrological cycle of ERA40, ERA40 Project Report Series, No. 24. European Centre for Medium Range Weather Forecasts. http://www.ecmwf@int

Hjellbrekke, A. G. 2001. Data report 1999. Acidifying and eutrophying compounds. Part 2: monthly and seasonal summaries. EMEP/CCC-Report 03/2001. Internet URL: http://www.nilu.no, 25 May 2005.

Huffman, G. J., Adler, R. F., Arkin, A., Chang, A., Ferraro, R. and co-authors. 1997. The Global Precipitation Climatology Project (GPCP) combined precipitation data set. *Bull. Amer. Meteor. Soc.* **78**, 5–20.

Jonson, J. E., Simpson, D., Fagerli, H. and Solberg, S. 2006. Can we explain the trends in European ozone levels? *Atmos. Chem. and Phys.* **6**, 51–66.

Kanakidou, M., Singh, H. B., Valentin, K. M. and Crutzen, P. J. 1991. A two dimensional study of ethane and propane oxidation in the troposphere. *J. Geophys. Res.* **96**(D8), 15 395–15 413.

Koutrakis, P., Wolfson, J. M., Spengler, J. D., Stern, B. and Franklin, C. A. 1989. Equilibrium size of atmospheric aerosol sulfates as a function of the relative humidity. *J. Geophys. Res.* **94**, 6442–6448.

Kovac, N., 2002. Mandatory data checking for the EMEP assessment. Environmental Agency of Slovenia, Monitoring office, air quality section, 2 pp. Internet URL: http://www.nilu.no/projects/ccc/sitedescriptions/si/index.html, 27 May 2005.

Kraus, K. B., Rohrer, F., Grobler, E. S. and Ehhalt, D. H. 1996. The global trorpspheric distribution of NO_x estimated by a three-dimensional chemical tracer model. *J. Geophys. Res.* **101**(D13), 18 587–18 604.

Kållberg, P. 1997. Aspects of the re-analysed climate *ECMWF Reanal. Proj. Rep. Ser.* **2**, 89. European Centre For Medium-Range Weather Forecasting, Geneva.

Langner, J., Bergström, R. and Pleijel, K. 1998. European scale modeling of sulphur, oxidized nitrogen and photochemical oxidants. Model

development and evaluation for the 1994 growing season, SMHI report, RMK No. 82, Swedish Met. and Hydrol. Inst., Norrköping, Sweden.

Langner, J., Bergström, R. and Foltescu, V. L. 2005. Impact of climate change on surface ozone and deposition of sulphur and nitrogen in Europe. *Atm. Env.* **39**, 1129–1141.

Lelieveld, J. and Dentener, F. 2000. What controls tropospheric ozone?. *J. Geophys. Res.* **105**(D3), 3531–3551.

Lövblad, G., Tarrason, L., Torseth, K. and Dutchak, S. (eds), 2004. EMEP Assessment, Part 1, European Perspective, EMEP MSC-W, Oslo, October 2004. URL: http://www.emep.int/index_assessment.html

Moxim, W. J., Levy, H. and Kasibhatla, P. S. 1996. Simulated global tropospheric PAN: Its transport and impact on NO_x. *J. Geophys. Res.* **101**(D7), 12 621–12 638.

Mårtensson, E. M., Nilsson, E. D., de Leeuw, G., Cohen, L. H. and Hansson, H.-C. 2003. Laboratory simulations and parametrization of the primary marine aerosol production. *J. Geophys. Res.* **108**(D9), doi:10.1029/2002JD002263.

Monahan, E. C., Spiel, D. E. and Davidson, K. L. 1986. A model of marine aerosol generation via whitecaps and wave disruption. In: *Oceanic Whitecaps and Their Role in Air-Sea Exchange* (eds E. C. Monahan and G. Mac Niocaill). D Reidel, Norwell, MA, pp. 167–174.

Näs, A., Moldanová, J., Lindskog, A., Bergström, R. and Langner, J. 2003. Identification and management of critical environmental impacts from air transportation over North Europe EIATNE. URL: http://www.eiatne.se/internt/FOI-S-1041-SE-EIATNE.pdf

Peters, W., Krol, M., Dentener, F. and Lelieveld, J. 2001. Identification of an El Niño-southern Oscillation signal in a multilayer global simulation of tropospheric ozone. *J. Geophys. Res.* **106**(D10), 10 389–10 402.

Quinn, T. L. and Ondov, J. M. 1998. Influence of temporal changes in relative humidity on dry deposition velocities and fluxes of aerosol particles bearing trace elements. *Atm. Env.* **32**, 3467–3479.

Robertson, L., Langner, J. and Engardt, M. 1999. An Eulerian limited-area atmospheric transport model. *J. Appl. Met.* **38**, 190–210.

Roemer, M., Beekman, M., Bergström, R., Boersen, G., Feldman, H., and co-authors. 2003. Ozone trends according to ten dispersion models, EUROTRAC-2, http://www.mep.tno.nl/eurotrac, click on EUROTRAC-trends.pdf.

Simmonds, P., Derwent, R., Manning, A. and Spain, G. 2004. Significant growth in surface ozone at Mace Head, Ireland 1987–2003. *Atm. Env.* **38**, 4769–4778.

Simmons, A. J., Jones, P. D., da Costa Bechtold, V.,Beljaars, C. M., Kållberg, P. W. and co-authors. 2004. Comparison of trends and low-frequency variability in CRU, ERA40, and NCEP/NCAR analyses of surface air temperature. *J. Geophys. Res.* **109**(D24), D24115, doi:10.1029/2004JD005306.

Simpson, D., Andersson-Sköld, Y. and Jenkin, M. E. 1993. Updating the chemical scheme for the EMEP MSC-W oxidant model: current status, EMEP MSC-W Note 2/93.

Simpson, D., Guenther, A., Hewitt, C. N. and Steinbrecher, R. 1995. Biogenic emissions in Europe. 1. Estimates and uncertainties.. *J. Geophys. Res.* **100**, 22 875–22 890.

Siniarovina, U. and Engardt, M. 2005. High-resolution model simulations of anthropogenic sulphate and sulphur dioxide in Southeast Asia. *Atm. Env.* **39**, 2021–2034.

Skjelkvåle, B. L., Evans, C., Larssen, T., Hindar, A. and Raddum, G. G. 2003. Recovery from acidification in European surface waters: A review to the future. *Ambio* **30**(3), 170–175.

Solberg, S., Bergström, R., Langner, J., Laurila, T., Sjöberg, K. and co-authors. 2002. Changes in ozone episodes due to emission reductions – A Nordic study. EMEP/CCC-Report 10/2002, Norwegian Institute for Air Research, P.O. Box 100, No-2027 Kjeller, Norway. URL: http://www.nilu.no/projects/ccc/reports/cccr10-2002.pdf

Solberg, S., Bergström, R., Langner, J., Laurila, T. and Lindskog, A. 2005a. Changes in Nordic ozone episodes due to European emission reductions in the 1990s. *Atm. Env.* **39**, 179–192.

Solberg, S., Derwent, R. G., Hov, Ø., Langner, J. and Lindskog, A., 2005b. European abatement of surface ozone in a global perspective. *Ambio* **34**(1), 47–53.

Stoddard, J. L., Jeffries, D. S., Lukeswille, A., Clair, T. A., Dillon, P. J. and co-authors. 1999. Regional trends in aquatic recovery from acidification in North America and Europe 1980–1995. *Nature* **40**, 575–578.

Svenningsson, B., Hansson, H.-C., Wiedensohler, A., Noone, K., Ogren, J. and co-authors. 1994. Hygroscopic growth of aerosol particles and its influence on nucleation scavenging in cloud: experimental results from Keiner Feldberg. *J. Atm. Chem.* **19**, 129–152.

Swietlicki, E., Zhou, J., Berg, O. H., Martinsson, B. G., Frank, G. and co-authors. 1999. A closure study of sub-micrometer aerosol particle hygroscopic behaviour. *Atm. Env.* **50**, 205–240.

Swietlicki, E., Zhou, J., Covert, D. S., Hämeri, K., Busch, B. and co-authors. 2000. Hygroscopic properties of aerosol particles in the north-eastern Atlantic during ACE-2. *Tellus* **52B**, 201–227.

Tilmes, S., Brandt, J., Flatøy, F., Bergström, R., Flemming, J. and co-authors. 2002. Comparison of five Eulerian air pollution forecasting systems for the summer of 1999 using the German ozone monitoring data. *J. Atm. Chem.* **42**, 91–121.

Tsyro, S. G. 2005. To what extent can water explain the discrepancy between model calculated and gravimetric PM_{10} and $PM_{2.5}$?. *Atmos. Chem. Phys.* **5**, 515–532.

Uppala, S., Kållberg, P., Hernandez, A., Saarinen, S., Fiorino, M. and co-authors. 2004. ERA40:ECMWF 45-year reanalysis of the global atmosphere and surface conditions 1957–2002. *ECMWF Newsletter* **101**, 2–21.

Uppala, S. M., Kållberg, P. W., Simmons, A. J., Andrae, U., da Costa Bechtold, V. and co-authors. 2005. The ERA40 re-analysis. *Quart. J. Roy. Met. Soc.* **131B**, 2961–3012.

van Loon, M., Roemer, M. G. M., Builtjes, P. J. H., Bessagnet, B., Rouil, L. and co-authors. 2004. Model inter-comparison. In the framework of the review of the unified EMEP model, TNO-report, TNO-MEP - R 2004/282, 53 pp.

Vestreng, V. 2003. EMEP/MSC-W Technical report. Review and Revision. Emission data reported to CLRTAP, MSC-W Status Report 2003. EMEP/MSC-W Note 1/2003. ISSN 0804-2446.

Zhang, L., Gong, S., Padro, J. and Barrie, L. 2001. A size-segregated particle dry deposition scheme for an atmospheric aerosol module. *Atm. Env.* **35**, 549–560.